Original Article

CYP1B1 promotes colorectal cancer liver metastasis by enhancing the growth of metastatic cancer cells via a fatty acids-dependent manner

Lei Jin[1#], Ju Huang[2#], Lei Guo[1#], Bo Zhang[1], Qin Li[2], Hui Li[1,3], Mincheng Yu[1], Peiyi Xie[1], Qiang Yu[1], Zheng Chen[1], Shuang Liu[4], Yongfeng Xu[1], Yongsheng Xiao[1], Ming Lu[2], Qinghai Ye[1]

[1]Department of Liver Surgery and Transplantation, Liver Cancer Institute, Zhongshan Hospital, Fudan University, Key Laboratory of Carcinogenesis and Cancer Invasion, Ministry of Education, Shanghai, China; [2]CAS Key Laboratory of Tissue Microenvironment and Tumor, Shanghai Institute of Nutrition and Health, Chinese Academy of Sciences, Shanghai, China; [3]Shanghai Medical College and Zhongshan Hospital Immunotherapy Technology Transfer Center, Shanghai, China; [4]Neurosurgery Department of Zhongshan Hospital, Fudan University, Shanghai, China

Contributions: (I) Conception and design: L Jin, J Huang; (II) Administrative support: M Lu, Q Ye; (III) Provision of study materials or patients: L Guo, B Zhang; (IV) Collection and assembly of data: L Jin, J Huang, L Guo; (V) Data analysis and interpretation: L Jin, J Huang, L Guo, Q Li; (VI) Manuscript writing: All authors; (VII) Final approval of manuscript: All authors.

[#]These authors contributed equally to this work.

Correspondence to: Ming Lu, PhD. CAS Key Laboratory of Tissue Microenvironment and Tumor, Shanghai Institute of Nutrition and Health, Chinese Academy of Sciences, 320 Yueyang Road, Shanghai 200031, China. Email: mlu@sinh.ac.cn; Qinghai Ye, PhD. Department of Liver Surgery and Transplantation, Liver Cancer Institute, Zhongshan Hospital, Fudan University, Key Laboratory of Carcinogenesis and Cancer Invasion, Ministry of Education, 180 Fenglin Road, Shanghai 200032, China. Email: ye.qinghai@zs-hospital.sh.cn.

Background: Liver metastasis (LM) accounts for most colorectal cancer (CRC)-related deaths. However, how metastatic CRC cells gain the ability to survive and grow in liver remains largely unknown.

Methods: First, we screened differentially expressed genes (DEGs) between LM and paired primary tumors (PTs) in Gene Expression Omnibus (GEO) database, and identified cytochrome P450 1B1 (*CYP1B1)* as the only common differential gene. Then, we verified messenger RNA (mRNA) and protein expression level in clinical specimens. After constructing stable up-regulated *CYP1B1* versions of HCT116 and RKO CRC cells and stable down-regulated CYP1B1 versions of SW480 and HT29 CRC cells, cell proliferation assays, subcutaneous tumor formation, and mouse LM models were used to comprehend its function. Next, we used RNA-seq to uncover specific mechanisms of growth; cell cycle, polymerase chain reaction (PCR), western blot (WB) and GEO series (GSE) datasets were used to verify its mechanism. Last, gas chromatography tandem mass spectrometry (GC-MS/MS) was adopted to examine which fatty acids were changed.

Results: A significantly higher level of CYP1B1 was found in LM than in PT in paired clinical CRC LM samples ($P<0.05$). After CYP1B1 overexpression in HCT116 and RKO cells, cell proliferation abilities *in vitro* and *in vivo* were enhanced; LM of NOD.Cg-Prkdc^{scid}Il2rg^{em1Smoc} (NSG) mice were enhanced. And knockdown of CYP1B1 in SW480 and HT29 cells, cell proliferation abilities *in vitro* and *in vivo* were reduced; LM of NSG mice were declined ($P<0.05$). RNA-seq showed 59 common genes from upregulated genes of RKO overexpression group and downregulated genes of SW480 knockdown group were enriched in cell cycle and DNA replication. Further investigation revealed CYP1B1 regulated alternation of *MCM5*, *PCNA*, and *FEN1* genes, and G1/S transition in CRC cells. GC-MS/MS revealed long chain fatty acids (LCFAs) made a difference in SW480 knockdown group ($P<0.05$). Through adding LCFAs into SW480 and HT29 knockdown groups, cell proliferation abilities *in vitro* and *in vivo* were enhanced, and expressions of *MCM5*, *PCNA*, *FEN1* were upregulated ($P<0.05$).

Conclusions: *CYP1B1* exerts a significant influence on LM of CRC by modulating tumor cell proliferation via "CYP1B1-LCFAs-G1/S transition". This finding suggests *CYP1B1* could be a promising target for CRC LM.

Keywords: Colorectal cancer (CRC); liver metastasis (LM); CYP1B1; cell cycle; fatty acids

Submitted Nov 08, 2023. Accepted for publication Dec 14, 2023. Published online Dec 27, 2023.
doi: 10.21037/jgo-23-895
View this article at: https://dx.doi.org/10.21037/jgo-23-895

Introduction

Metastasis is an intricate multistep process involving dissemination of primary cancer cells, survival of disseminated tumor cells (DTCs) in circulation, colonization, and the subsequent proliferation of DTCs in a distant metastatic organ. Among these steps, metastatic colonization is the most complex and rate-limiting phase of metastasis (1). However, the mechanism underlying how DTCs gain the ability to colonize and to grow in the hostile metastatic environments remains elusive.

Metabolic reprogramming is an emerging hallmark of cancer, and cancer cells are known to undergo metabolic alterations to sustain faster proliferation (2). A recent study has shown that DTCs undergo specific metabolic adaptations which enable them to colonize and grow in distinct metastatic organs (3). Therefore, clarifying the key genes and mechanisms underlying metabolic adaptations in metastatic organs might provide potential therapeutic strategies against cancer metastasis.

Colorectal cancer (CRC) is one of the most common malignant cancers worldwide (4). Metastasis is the major cause for high mortality of CRC, and the liver is the most common metastasis organ of CRC (5). In clinical practice, about half of CRC patients have liver metastasis (LM), and the main treatments include surgical resection, radiotherapy, chemotherapy, and combination therapy. However, about 80% of CRC patients develop resistance to these therapies (6,7).

Cytochrome P450 1B1 (*CYP1B1*) is a member of the cytochrome P450 family. It mainly participates in the metabolism of various exogenous and endogenous substrates, including fatty acids, arachidonic acid, steroid hormones, and vitamins, among others (8). For example, *CYP1B1* can hydroxylate estrone (E1) and 17β-estradiol (E2) to 2- and 4-hydroxy estrone E2, the latter are further transformed into quinones to form DNA adducts resulting in carcinogenic mutations (9); and *CYP1B1* can affect blood pressure fluctuation via influencing Ang II expression, this mechanism is achieved by influencing arachidonic acid (AA) metabolism (10). The expression of CYP1B1 is regulated by various factors, including aromatic hydrocarbon receptor (AhR), AhR/AhR nuclear translocation complex (ARNT), estrogen receptor (ER), and so on (11).

CYP1B1 is closely related to cancer. In inflammatory breast cancer, upregulation of *CYP1B1* is caused by Wnt5a/b and β-catenin activation, resulting in a worse clinical prognosis (12). In prostate cancer, *CYP1B1* catalyzes 4-hydroxy-E2 to enhance IL6-STAT3 signaling, which results in male androgen deprivation resistance and decreases bicalutamide sensitivity (13). In CRC, via the activation of the JAK/PI3K/AKT pathway, the methylation of CpG island near miR-27b regulates *CYP1B1* to promote the evolution of CRC (14). Another article found that *CYP1B1* is highly expressed in patients with distant metastasis of colorectal adenocarcinoma (COAD), however, the specific mechanism is unclear (15). Based on the above research progress, investigating latest mechanisms of *CYP1B1* in CRC hepatic metastasis is being urgent. In this study, we analyzed the differentiated genes from four published Gene Expression Omnibus (GEO) datasets, and identified *CYP1B1* as a common upregulated gene in LM of CRC compared with primary tumors (PTs). *CYP1B1*

Highlight box

Key findings
- The mRNA and protein levels of *CYP1B1* were significantly higher in liver metastasis (LM) than in primary tumor (PT) in paired clinical colorectal cancer (CRC) liver metastatic samples.
- *CYP1B1* exerts a significant influence on LM of CRC by modulating tumor cell proliferation via "CYP1B1-LCFAs-G1/S transition".

What is known and what is new?
- Many factors are involved in LM of CRC. *CYP1B1* is a member of the cytochrome P450 family, which is closely related to cancer.
- In this study, we found *CYP1B1* was highly expressed in LM of CRC. It can facilitate G1/S transition of CRC cells and promote CRC cell growth by enhancing fatty acids biosynthesis.

What is the implication, and what should change now?
- Targeting "CYP1B1-LCFAs-G1/S transition" may inhibit the progression of LM of CRC, and may provide a new idea for the treatment of LM.

was found to promote CRC cell proliferation *in vitro* and CRC LM *in vivo*. Further mechanistic studies revealed that *CYP1B1* facilitated G1/S transition of CRC cells via enhancing fatty acids biosynthesis. We present this article in accordance with the ARRIVE reporting checklist (available at https://jgo.amegroups.com/article/view/10.21037/jgo-23-895/rc).

Methods

Animals

Male, BALB/c and NOD.Cg-Prkdc^{scid}Il2rg^{em1Smoc} mice, 4–6 weeks old, were purchased from Shanghai Model Organisms. Animals were housed under specific-pathogen-free conditions in Shanghai Institute of Nutrition and Health, CAS (Shanghai, China). Animal experiments were treated in strict accordance with animal care procedures and methods approved by Institutional Animal Care and Use Committee at Shanghai Institute of Nutrition and Health, Chinese Academy of Sciences (No. SINH-2022-LM-1). Experiments were in compliance with Chinese National Standard (GBT35823-2018) for the care and use of animals. A protocol was prepared before the study without registration.

Patient specimens

A total of 21 paired CRC tissues and paired LM [9 paired tissues were used for real-time quantitative polymerase chain reaction (qRT-PCR) analysis and 12 paired tissues were used for immunohistochemistry (IHC) analysis] were acquired from CRC patients who accepted homochromous colectomy and hepatic resection from 2005 to 2015 with informed consent based on ethical standards of Institutional Review Board in Zhongshan Hospital of Fudan University (No. B2020-348R), China. The study was conducted in accordance with the Declaration of Helsinki (as revised in 2013).

Cell culture

CRC cell lines [HCT116 (#TCHu99), RKO (#TCHu116), SW480 (#TCHu172), and HT29 (#TCHu103)] were obtained from Cell Bank of Chinese Academy of Sciences (https://www.cellbank.org.cn/; Shanghai, China). HT29 cells were cultured or maintained in Roswell Park Memorial Institute (RPMI)-1640 (Gibco, Billings, MT, USA) supplemented with 10% fetal bovine serum (FBS) at 37 ℃ in 5% CO_2. Other cell lines were cultured or maintained in Dulbecco's modified Eagle medium (DMEM) (Gibco) supplemented with 10% FBS at 37 ℃ in 5% CO_2.

Antibodies or reagents

The primary antibodies included anti-CYP1B1 (#abs115548, Absin, Shanghai, China; #18505-1-AP, Proteintech, Rosemont, IL, USA), anti-MCM5 (#T57185, Abmart, Berkeley Heights, NJ, USA), anti-FEN1 (#T56956, Abmart), anti-β-Actin (#sc-47778, Santa Cruz), anti-GAPDH (#sc-47724, Santa Cruz), and anti-PCNA (#sc-56, Santa Cruz Biotech., Dallas, TX, USA). Fatty acid synthetase inhibitors C75 was purchased from MedChemExpress (MCE, Monmouth Junction, NJ, USA; #HY-12364), cis-11-Eicosenoic acid (C20:1), cis-8,11,14-Eicosatrienoic acid (C20:3) were purchased from Sigma (Sigma Aldrich, St. Louis, MO, USA; #E3635, E4504), and arachidic acid (C20:0) was purchased from Aladdin (Shanghai, China; #A110476).

Measurement of fatty acids

Free fatty acids (FFAs) were detected by Free Aliphatic Acid Assay Kit (#AK230, Bioss Antibodies, Woburn, MA, USA). Briefly, after the confluent cells (fully grown in a 6 cm culture dish) were washed twice with phosphate-buffered saline (PBS), 300 µL palmitic acid (5 µmol/mL, dissolved in chloroform) was added and the cells were homogenized. The mixture was then centrifuged at 8,000 rpm, 4 ℃ for 10 minutes, and the supernatant was collected for further analysis. Following the protocol instructions, reagents were added sequentially, and the absorbance value was measured at 550 nm to convert to FFA content.

IHC and evaluation of the IHC staining

IHC staining was carried out using a 2-step protocol (Novolink Polymer Detection System; Novocastra, Newcastle upon Tyne, UK) on the basis of the manufacturer's instructions. After antigen retrieval, the slides were incubated with antibodies at 4 ℃ overnight. Next, the slides were incubated with secondary antibody (GK500705; Genetech, San Francisco, CA, USA) at 37 ℃ for 30 minutes. Then, slides were incubated in a 3,3-diaminobenzidine solution and counterstained with Mayer's hematoxylin. Negative controls from all assays were included without primary antibodies. IHC staining was assessed by three independent pathologists without comprehension of the pathologic and clinical features of the cases. Any discrepancies were resolved by consensus. We captured three representative microscope fields using the Leica QWin Plus v3 software (Leica, Wetzlar, Germany), with identical settings used for each photograph. The staining score was evaluated with a range of 1 to 4 according to the percentage of tinct tumor cells and the staining intensity. Final IHC score was calculated by the sum of 4 × (% 4) + 3 × (% 3) + 2 × (% 2) + 1 × (% 1).

Analysis of GEO datasets

Gene expression profiles of CRC tissues and LM of CRC were downloaded from GEO database. The independent datasets of GSE14297, GSE41258, GSE49355, and GSE40367 were analyzed, which contained 18 paired, 5 paired, 13 paired, and 7 paired PT and LM, respectively. Data were first transformed using $\log_2$ and then normalized using the Quantile method; The "edgeR" (https://www.r-project.org/) was used to perform differential analysis between the PT and LM. Genes that met the criteria of |foldchange| >1.5 and adjusted P value <0.05 were considered to have significant differences. A volcano plot was generated to display messenger RNA (mRNA) profiles by the "ggplot" package (https://mirrors.tuna.tsinghua.edu.cn/CRAN/web/packages/ggplot2/index.html). The differentially expressed genes (DEGs) in 4 datasets were then screened using online Venn (https://bioinformatics.psb.ugent.be/webtools/Venn/). The expression value of DEGs extracting from normalized GEO series (GSE) datasets were mapped by GraphPad Prism (version 8.0; GraphPad Software, San Diego, CA, USA). Analysis of PT and normal colon tissues (NC) revealed that there were 7 paired samples in GSE14297, 43 paired samples in GSE41258, and 15 paired samples in GSE49355 (no paired samples in GSE40367), respectively. The specific procedure was similar with the above process.

RNA extraction, RT-PCR, and qRT-PCR

Total RNA from cells or tissues was extracted using TRIzol reagent (Invitrogen, Carlsbad, CA, USA) and reverse-transcribed to complementary DNA (cDNA) using the Prime Script™ RT Reagent Kit (Takara Bio, Dalian, China). Gene expression was analyzed in triplicate by the Applied Biosystems 7900 HT Fast Real-Time PCR System (Applied Biosystems, Waltham, MA, USA). Relative expression of each gene was calculated by $2^{-\Delta\Delta Ct}$ method after β-actin normalization. The primers used for qRT-PCR are listed in Table S1.

Western blotting

RIPA buffer with 1% protease inhibitor was used for lysate preparation. A bicinchoninic acid assay kit (Pierce; Thermo Fisher Scientific, Inc., Waltham, MA, USA) was used for measuring protein concentration. A total of 200 µg per well was electrophoresed in 10% sodium dodecyl sulfate-polyacrylamide gels and transferred onto polyvinylidene fluoride (PVDF) membranes. Next, the PVDF was blocked with 5% fat-free milk at room temperature for 1 hour, then, the membranes were incubated with primary antibody at 4 ℃ overnight. Next, the membranes were washed with tris-buffered saline with Tween 20 (TBST) and incubated with horseradish peroxidase (HRP)-conjugated secondary antibodies for 2 hours at room temperature. Antibody binding was exposed by enhanced chemiluminescence western blotting substrate (Pierce; Thermo Fisher Scientific, Inc., Rockford, IL, USA).

Lentivirus-mediated gene knockdown or overexpression

For lentivirus generation, 1×10^7 293T cells were cultured in a 10 cm dish in DMEM containing 10% FBS the day before transfection. Cells were then transfected by changing to 10 mL of DMEM containing 16 mL of Lipofectamine 2000 (#11668027, Thermo Fisher Scientific), 4 mg of knockdown plasmid or overexpressed plasmid combined with 3 mg psPAX2 and 1 mg pMD2. G. After 6 hours, the media was changed with DMEM with 10% FBS. The supernatant was collected 48 hours later, after filtering with 0.45 mm filters, they were used to infect CRC cell lines. The stable cell lines were acquired by puromycin intervention 1 week later. The short hairpin RNA (shRNA) target sequences were as follows: Sh-h-CYP1B1-1: CCCAAGTCATTTAAAGTCAAT; Sh-h-CYP1B1-2: CAGCAACTTCATCCTGGACAA.

Cell proliferation

Cells (100 µL aliquots) were cultured in 96-well plates at a density of 2,000–5,000 cells/well, and 10 µL Cell Counting Kit-8 (CCK-8) solution (Dojindo, Kumamoto, Japan) was added at the indicated time points. Cell viability was determined by measurement of absorbance at indicated time.

Cell cycle analysis

Cells (1×10^6) were seeded in 6-well plates, when the growth reached 75–85% density (24–36 h), cells were collected by trypsinization, centrifuged at 1,000 g for 3 minutes, and fixed in 70% ethanol at −20 ℃ overnight. After that, cells were centrifuged at 1,000 g for 3 minutes before being washed and resuspended with 1 mL of PBS twice, resuspended in 500 µL propidium iodide (PI)/Rnase staining buffer, incubated for 40 minutes at 37 ℃, and analyzed using flow cytometry within 2 hours. The cellular DNA content was performed using an A1711 Analytical flow cytometer (Beckman Coulter, Brea, CA, USA). Acquired data were analyzed utilizing Flowjo Software (Becton, Dickinson, and Co., Ashland, OR, USA).

Tumor xenograft mouse model

HCT116-Control, RKO-Control, SW480-shNT, HT29-shNT, and their corresponding stable transfected cell lines (1×10^6/100 µL PBS) were subcutaneously implanted into the dorsal right flank of nude mice to establish subcutaneous tumor models. Tumor weights were measured on indicated days by electronic scales.

To establish intra-splenic injection models, RKO or SW480 corresponding stable transfected cells (1×10^6/100 µL PBS) were injected into the spleen of NOD. Cg-Prkdc^{scid}Il2rg^{em1Smoc} mice and observed for 4 weeks. At the end of each process (about 4 weeks), mice were executed, and tumors were isolated, weighed, photographed, and used for diverse experiments.

Final verification of arachidic acid (C20:0) on tumorigenesis was conducted. The steps were similar after co-culture with corresponding cells for 48 hours.

RNA sequencing and data analysis

Total RNA was extracted using the TRIzol reagent (Invitrogen) based on the manufacturer's protocol. RNA quantification and purity were estimated using the NanoDrop 2000 spectrophotometer (Thermo Scientific). RNA integrity was analyzed using the Agilent 2100 Bioanalyzer (Agilent Technologies, Santa Clara, CA, USA). Then, the libraries were structed using VAHTS Universal V6 RNA-seq Library Prep Kit (Illumina, San Diego, CA, USA) on the basis of manufacturer's instructions. The libraries were sequenced on an Illumina Novaseq 6000 platform and 150 bp paired-end reads were generated. Raw reads of fastq format were firstly processed using fastp (16) and low-quality reads were removed to obtain the clean reads. The clean reads were mapped to the reference genome using HISAT2 (17). Fragments per kilobase per million (FPKM) of each gene was counted and the read counts of each gene were acquired by HTSeq-count (18). Principal component analysis (PCA) was conducted using R (v 3.5.1; R Foundation for Statistical Computing, Vienna, Austria) to estimate the biological duplication of samples. Differential expression analysis was conducted using the DESeq2 (19). |foldchange| >1.5 and Q value <0.05 was set as the threshold for significantly DEGs. Based on the hypergeometric distribution, Gene Ontology (GO), Kyoto Encyclopedia of Gene sand Genomes (KEGG) pathway, KEGG map, Reactome, and WikiPathways enrichment analysis of DEGs were performed to screen the significant enriched term using "enrichplot" package (https://bioconductor.org/packages/release/bioc/html/enrichplot.html) or "clusterProfiler" package (https://bioconductor.org/packages/release/bioc/html/clusterProfiler.html). The data presented in our study were deposited in the GEO repository, series record GSE232193.

Gas chromatography (GC) tandem mass spectrometry

The GC analysis was performed on a trace 1300 gas chromatograph (Thermo Fisher Scientific). The GC was fitted with a capillary column Thermo TG-FAME (50 m × 0.25 mm ID × 0.20 µm) and helium was used as the carrier gas at 0.63 mL/min. Injection was made in split mode at 8:1 with an injection volume of 1 µL and an injector temperature of 250 ℃. The temperature of MS transfer line and ion source was 280 and 300 ℃, respectively. The column temperature was programmed to increase from an initial temperature of 80 ℃, which was maintained for 1 minute, followed by an increase to 160 ℃ at 20 ℃/min, which was maintained for 1.5 minutes, then an increase to 196 ℃ at 3 ℃/min, which was maintained for 8.5 minutes, and finally to 250 ℃ at 20 ℃/min and kept at this temperature for 3 minutes. Mass spectrometric detection of metabolites was conducted on TSQ 9000 (Thermo Fisher Scientific) with electron impact ionization mode. Single ion monitoring (SIM) mode was performed with the electron energy of 70 eV (20,21).

Statistical analysis

Statistical analysis was conducted using SPSS 24.0 (IBM Corp., Armonk, NY, USA) and GraphPad Prism 8.0 software. All experiments were performed at least 3 times, and results were presented as the mean ± standard deviation (SD) or mean ± standard error of the mean (SEM) (specific application see figure legends). The statistically significant changes were indicated with asterisk (*P<0.05, **P<0.01, ***P<0.001).

Results

CYP1B1 is highly expressed in LM of CRC

To identify the key genes involved in colonization and outgrowth of metastatic CRC cells in the liver, matched samples (PTs and LMs) of CRC patients from four National Center for Biotechnology Information (NCBI) GEO datasets (GSE14297, GSE40367, GSE41258, GSE49355) were selected, and the transcriptomic profiles of these samples of each GEO dataset were obtained and processed by standard GEO2R analysis, followed by $\log_2$ transformation and quantile normalization. Paired differential analysis comparing matching PT and LM identified a set of DEGs which are up-regulated in LM for each of the four GEO datasets (Figure S1A-S1D). By overlapping the four groups of up-regulation genes, we identified a single up-regulated gene *CYP1B1* (*Figure 1A*,*1B*). We then analyzed the expression of *CYP1B1* by using independent paired CRC tissue samples, and the results confirmed that both CYP1B1 mRNA (*Figure 1C*) and protein (*Figure 1D*,*1E*) levels were apparently higher in LM of CRC than in those in paired PT. Moreover, the expression of *CYP1B1* did not show remarkable difference between PT and paired normal colon tissues in CRC patients (Figure S1E), hinting that up-regulation of CYP1B1 does not occur in the PT stage. These results indicate that CYP1B1 is highly expressed in LM of CRC.

CYP1B1 promotes cell proliferation of CRC cells in vitro and in vivo

Next, to determine the function of *CYP1B1* in the *in vitro* proliferation of CRC cells, we first examined the expression of *CYP1B1* in different CRC cell lines, and found that *CYP1B1* was highly expressed in HT29 cells, and was expressed at very low level in RKO cells and at intermediate levels in HCT116 and SW480 cells (*Figure 2A*,*2B*). Then, we overexpressed *CYP1B1* in HCT116 and RKO cells (*Figure 2C*,*2D* and Figure S2A,S2B), and generated two *CYP1B1*-specific shRNAs to silence the *CYP1B1* expression (shCYP1B1) in SW480 cells and HT29 cells (*Figure 2E*,*2F* and Figure S2C,S2D). Overexpression of *CYP1B1* significantly enhanced the cell proliferation of HCT116 cells (*Figure 2G*) and RKO cells (*Figure 2H*), whereas knockdown of *CYP1B1* resulted in a dramatic inhibition of *in vitro* cell proliferation of both SW480 (*Figure 2I*) and HT29 cells (*Figure 2J*). We further confirmed the role of *CYP1B1* in tumor growth *in vivo*. In subcutaneous xenograft models, overexpression of *CYP1B1* significantly increased tumor growth (*Figure 2K*,*2L*), whereas knockdown of *CYP1B1* led to a dramatic inhibition of tumor growth (*Figure 2M*,*2N*). These results indicated that *CYP1B1* promotes cell proliferation of CRC cells *in vitro* and *in vivo*.

CYP1B1 promotes CRC LM

To investigate the role of *CYP1B1* in CRC LM, especially in the colonization and outgrowth of CRC cells in liver, we established an experimental CRC LM model by intrasplenic injection of RKO control cells and *CYP1B1* overexpressed RKO cells or SW480 shNT (SW480 stably transfected with non-target shRNA control) cells and SW480 shCYP1B1 cells in NOD.Cg-Prkdc^{scid}Il2rg^{em1Smoc} (NSG) mice (*Figure 3A*). The results showed that both the number and the size of LM of the *CYP1B1* overexpression group were obviously increased compared with those of the control group (*Figure 3B-3E*). In addition, IHC staining showed that overexpression of *CYP1B1* was maintained in LM (*Figure 3F*). Silencing *CYP1B1* resulted in significant reduction of both the number and the size of LM (*Figure 3G-3K*). These results demonstrate that manipulating *CYP1B1* significantly affects the growth of CRC LM *in vivo*.

CYP1B1 facilitates G1/S transition of CRC cells

Next, to reveal the mechanism underlying the pro-metastasis effect of *CYP1B1*, we performed RNA sequencing to identify the potential transcriptional targets of *CYP1B1* in RKO and SW480 cells. The results showed that there were 1,104 genes with a statistically significant difference of 1.5-fold or more between RKO control cells

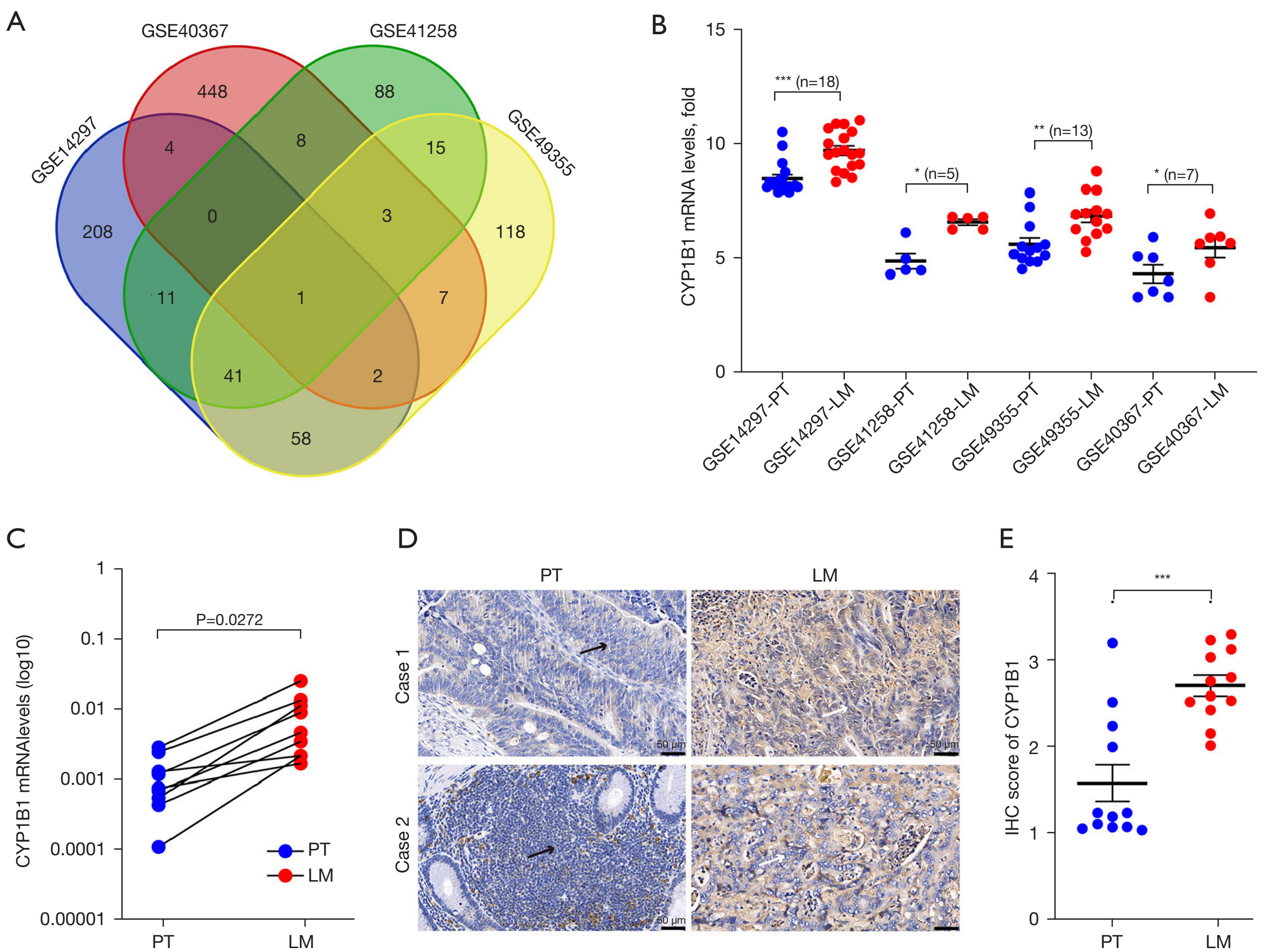

Figure 1 *CYP1B1* is highly expressed in liver metastases of colorectal cancer. (A) Venn diagram depicting the overlapping up-regulated genes in LM compared with those in paired CRC PTs from four GSE databases (GSE14297, GSE40367, GSE41258, GSE49355). (B) The CYP1B1 mRNA levels in PT and LM from four GSE databases. Each dot represents the relative mRNA level in PT or LM in each tissue sample from four GSE databases, data are shown as mean ± SEM. (C) Quantitative RT-PCR analysis of mRNA levels for *CYP1B1* in paired CRC samples (n=9). (D,E) Representative IHC pictures of CYP1B1 protein in paired CRC samples (left of D). The IHC score of CYP1B1 is shown in (E), data are shown as mean ± SEM (n=12). Scale bar, 50 μm. Black arrow points to PT from colon tissue, white arrow points to LM from liver tissue. Significance was determined by a 2-tailed paired *t*-test. *, P<0.05; **, P<0.01; ***, P<0.001. mRNA, messenger RNA; PT, primary tumor; LM, liver metastases; IHC, immunohistochemistry; CRC, colorectal cancer; GSE, GEO series; SEM, standard error of the mean; RT-PCR, real-time polymerase chain reaction.

and *CYP1B1* overexpression RKO cells, among which 494 were up-regulated and 610 were down-regulated (Figure S3A). There were 4,049 genes with a statistically significant difference of 1.5-fold or more between SW480-shCYP1B1 and SW480-shNT, among which 2,046 were up-regulated and 2,003 were down-regulated (Figure S3A). By overlapping the up-regulation genes in *CYP1B1* overexpression RKO cells and the down-regulation genes in SW480 shCYP1B1 cells, 59 common DEGs were obtained (*Figure 4A*). We then performed enrichment analysis on these 59 genes, including GO/KEGG analysis, WikiPathway enrichment analysis, and Reactome enrichment analysis. The results showed that the most enriched pathway was the cell cycle and DNA replication, which includes the *MCM2*, *MCM3*, *MCM5*, *PCNA*, *FEN1*, and *LIG1* genes (*Figure 4B* and Figure S3B-S3G). The

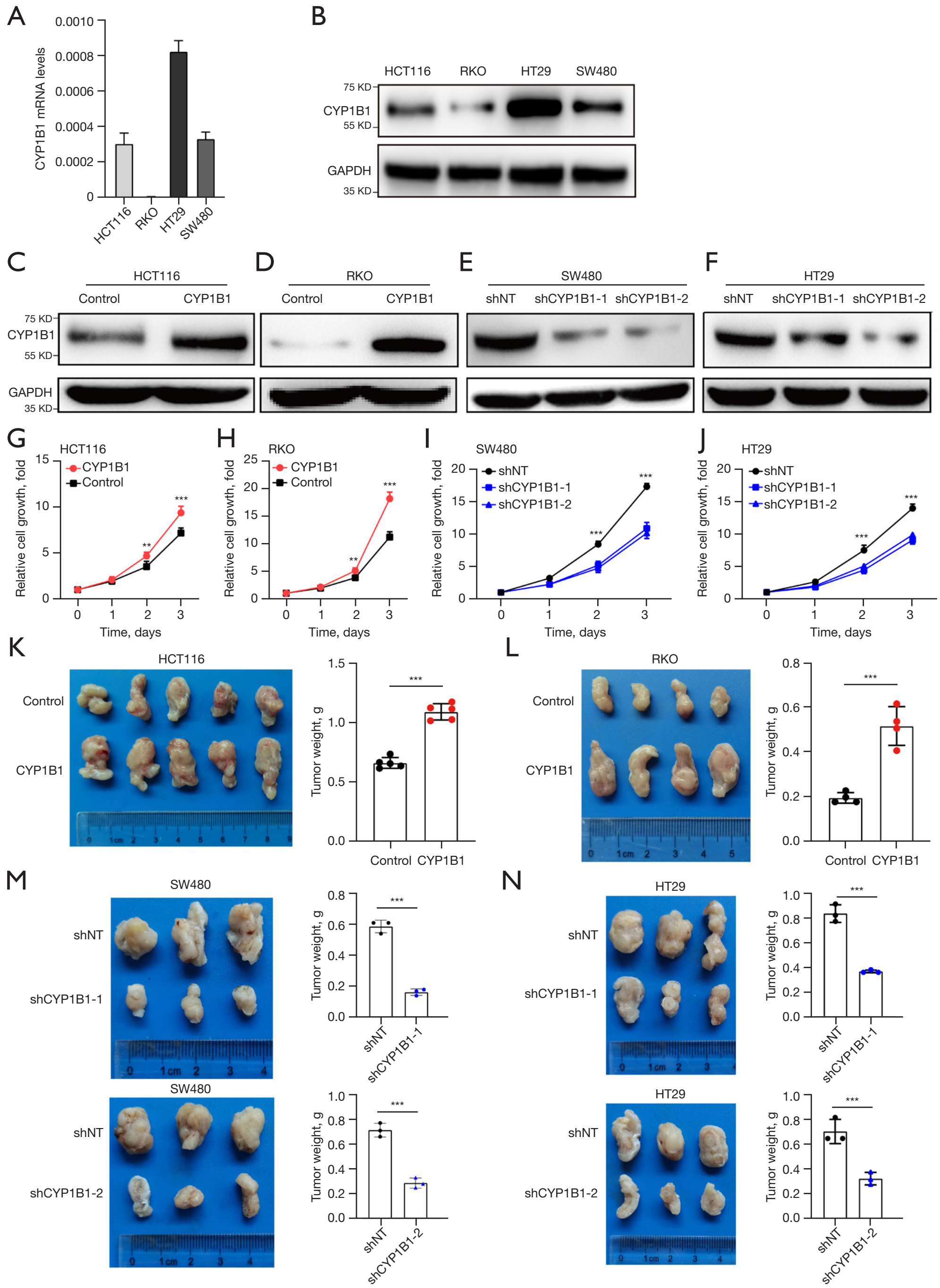

Figure 2 *CYP1B1* promotes cell proliferation of CRC cells *in vitro* and *in vivo*. (A,B) Expression of *CYP1B1* in human CRC cell lines determined by quantitative RT-PCR (A) or western blotting (B), data are shown as mean ± SD for (A). (C-F) Confirmation of *CYP1B1* overexpression and knockdown in CRC cell lines. The expression of *CYP1B1* was determined by western blotting. (G-J) The effects of *CYP1B1* overexpression or knockdown on cell proliferation of CRC cell lines. The relative cell number is expressed as fold change to day 0, data are shown as mean ± SD of quinary experiments. (K-N) The effects of *CYP1B1* overexpression or knockdown on tumor growth of CRC xenograft tumors. Tumor weight was assessed on the indicated days (4 weeks after injection) and tumors were dissected for photo in the left of (K-N), data are shown as mean ± SD. Significance was determined by 2-way ANOVA (G-J) or Student's *t*-test (K-N). **, P<0.01; ***, P<0.001. mRNA, messenger RNA; shNT, non-target shRNA control; CRC, colorectal cancer; RT-PCR, real-time polymerase chain reaction; SD, standard deviation; ANOVA, analysis of variance.

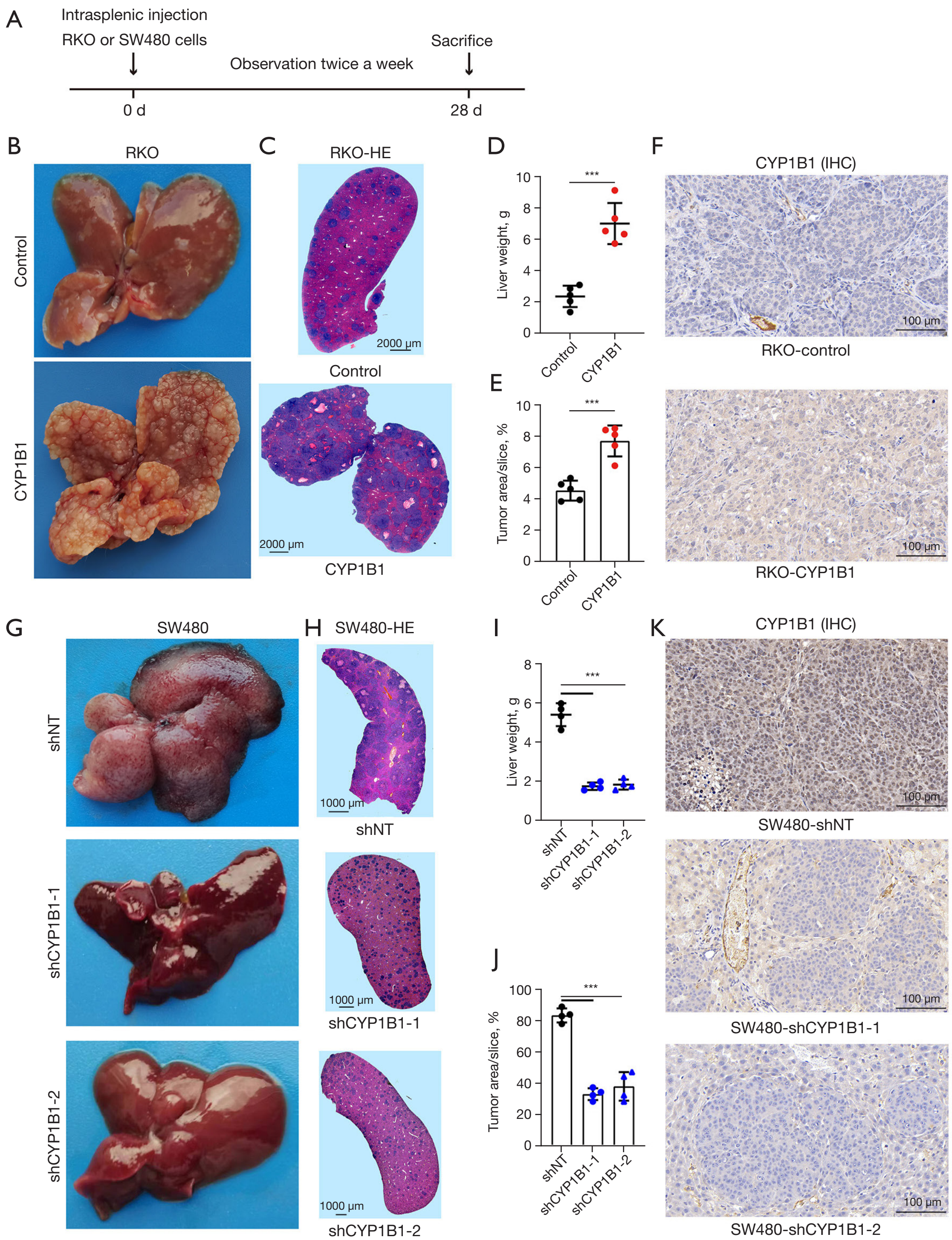

Figure 3 *CYP1B1* promotes liver metastases of CRC cells *in vivo*. (A-K) The effect of *CYP1B1* overexpression (n=5) or knockdown (n=4) on CRC liver metastases in intrasplenic injection model. The whole flow chart is pressed in (A). At the end of the experiment, liver was taken photos (B,G), for H&E staining (C,H), dissected for assessing liver weight (D,I) and tumor proportion of liver (E,J), and IHC staining of CYP1B1 protein (F,K). For (C): scale bar, 2,000 μm; for (H): scale bar, 1,000 μm; for (F,K): scale bar, 100 μm. For (D,E,I,J): data are shown as mean ± SD. Significance was determined by Student's *t*-test (D,E) or one-way ANOVA (I,J). ***, P<0.001. shNT, non-target shRNA control; IHC, immunohistochemistry; CRC, colorectal cancer; H&E, hematoxylin and eosin; ANOVA, analysis of variance.

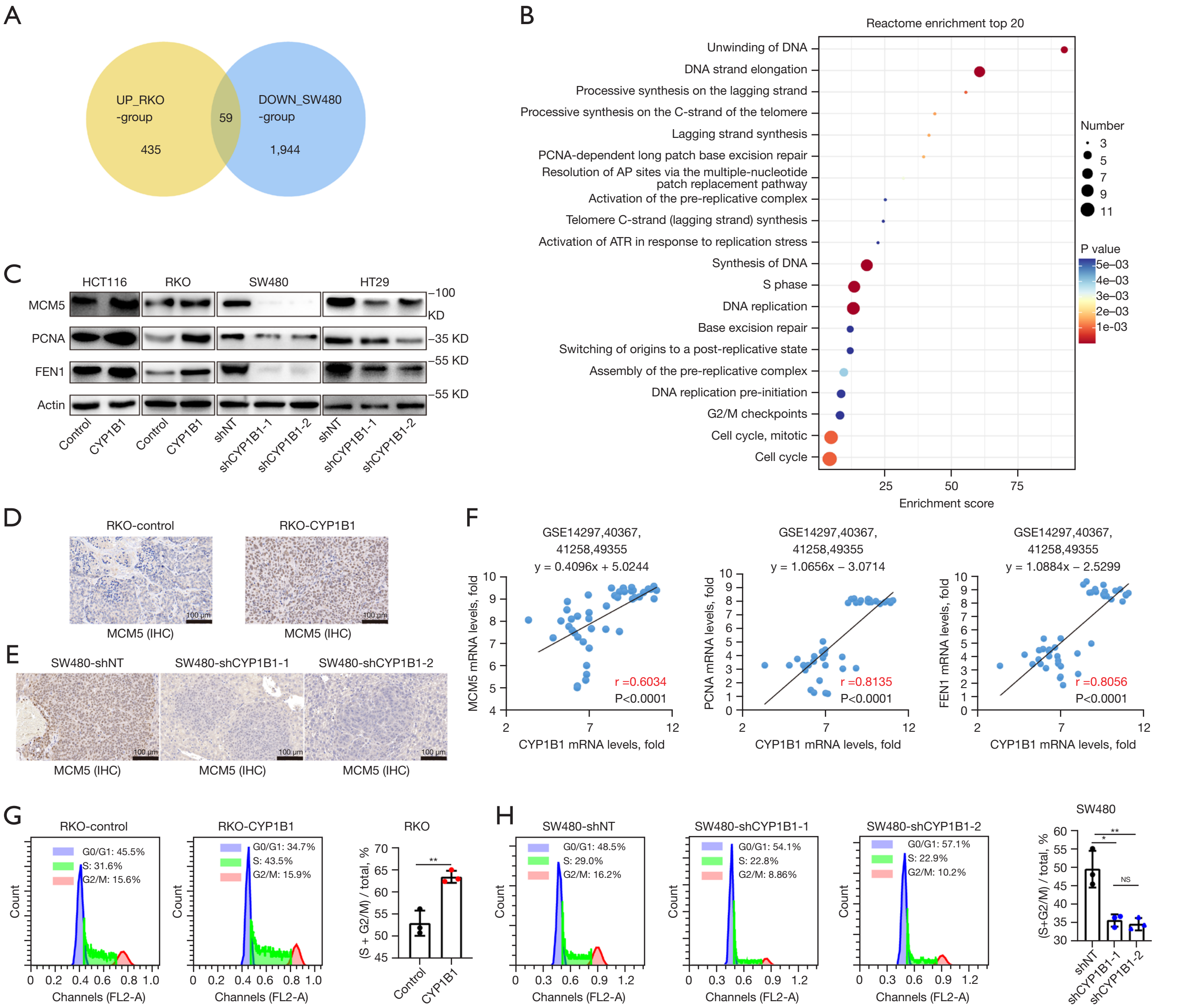

Figure 4 *CYP1B1* facilitates CRC cell growth by regulating G1/S transition. (A-C) Gene expression profiles were analyzed by RNA sequencing in indicated cell lines. Overlapping of genes resulting from comparison of up-regulated genes in RKO cells after overexpression of *CYP1B1* and down-regulated genes in SW480 cells after knockdown of *CYP1B1* are shown in (A). Reactome enrichment of overlapping differentiated genes (A) are shown in (B). (C) Growth-related genes were verified in CRC cell lines by western blotting. *MCM5*, *PCNA*, and *FEN1* showed consistent tendency in CRC cells after CYP1B1 intervention. (D,E) Representative IHC pictures of MCM5 in liver metastases samples from intrasplenic injection models of RKO (D) and SW480 cells (E). Scale bar, 100 µm. (F) Correlations between the expression of CYP1B1 gene and the expressions of *MCM5*, *PCNA*, and *FEN1* in 4 GSE databases (GSE14297, GSE40367, GSE41258, GSE49355). The mRNA levels of *CYP1B1*, *MCM5*, *PCNA*, and *FEN1* were obtained from 4 GSE databases, and were normalized and made correlation analysis. (G,H) Cell cycle analysis of RKO and SW480 group cells by flow cytometry. The proportion of proliferative cells after *CYP1B1* overexpression in RKO cell is shown in right of (G), the proportion of proliferative cells after *CYP1B1* knockdown in SW480 cell is shown in right of (H). Representative results from at least 3 independent experiments are shown, data are shown as mean ± SD. Significance was determined by Student's *t*-test (G), one-way ANOVA (H), Pearson correlation coefficients (F). *, P<0.05; **, P<0.01. NS, not significant as indicated. IHC, immunohistochemistry; mRNA, messenger RNA; shNT, non-target shRNA control; CRC, colorectal cancer; GSE, GEO series; SD, standard deviation; ANOVA, analysis of variance.

expression of these candidate genes was then validated in an independent CRC cell sample set (*Figure 4C* and Figure S4). Notably, the expressions of the *MCM5*, *PCNA*, and *FEN1* genes were up-regulated when *CYP1B1* was overexpressed, and were down-regulated when CYP1B1 was knocked down (*Figure 4C*). Similar results were obtained by using LM samples from intrasplenic injection models of CRC in *Figure 3* (*Figure 4D,4E*). Finally, the expression of *CYP1B1* also showed positive correlation with those of the *MCM5*, *PCNA*, or *FEN1* genes in human CRC LM samples from the 4 GEO datasets used above (*Figure 4F*).

As *MCM5*, *PCNA*, and *FEN1* genes are key players in cell cycle regulation, we further examined the effect of manipulating *CYP1B1* on cell cycle in CRC cells by flow cytometry. After *CYP1B1* overexpression, there was an obvious increase in the number of cells in S phase (31.6% in control cells *vs.* 43.5% in overexpression cells) and a decrease in the number of cells in G0 and G1 phases (*Figure 4G*). Conversely, after *CYP1B1* silencing, there was an obvious decrease in the number of cells in S phase (29.0% in SW480 shNT cells *vs.* 22.8 and 22.9% in 2 knockdown cells) and an increase in the number of cells in G0 and G1 phases (*Figure 4H*). The results above demonstrate that *CYP1B1* promotes G1/S transition of CRC cells.

CYP1B1 promotes CRC cell growth by enhancing fatty acids biosynthesis

Previous articles have shown that *CYP1B1* has an important role in fatty acids metabolism (8). Therefore, we determined the effects of manipulating *CYP1B1* on the FFA levels in CRC cells. The results showed that after *CYP1B1* overexpression, FFA levels were significantly increased, whereas FFA levels were significantly decreased after knockdown of *CYP1B1* (*Figure 5A-5D*), indicating that *CYP1B1* enhances FFA biosynthesis. Next, to explore whether FFA biosynthesis is required for *CYP1B1*-induced CRC cell growth, we used C75, the inhibitor of fatty acid synthase, to treat *CYP1B1* overexpressing CRC cells. The results showed that C75 treatment reversed the pro-growth effect of *CYP1B1* in RKO cells (*Figure 5E*) and HCT116 cells (*Figure 5F*). Meanwhile, C75 treatment did not affect the cell growth of RKO control cells and HCT116 control cells (*Figure 5E,5F*). Subsequently, we examined the effects of FFA biosynthesis inhibition on the expression of *CYP1B1*-regulated genes involved in G1/S transition, and found that C75 treatment significantly suppressed the elevated expression of *MCM5*, *PCNA*, and *FEN1* in *CYP1B1*-overexpressed RKO cells to levels similar to that of RKO control cells (*Figure 5G* and Figure S5A-S5C). Similar results were obtained by using HCT116 cells (*Figure 5H* and Figure S5D-S5F). Collectively, these data demonstrate that *CYP1B1* promotes CRC cell growth by enhancing fatty acids biosynthesis.

Long chain fatty acids (LCFAs) up-regulate the expression of MCM5, PCNA, and FEN1

To further determine the specific fatty acids responsible for the pro-growth effect of *CYP1B1*, we analyzed the levels of medium-chain and LCFAs by gas chromatography tandem mass spectrometry (GC-MS/MS) in SW480 shNT and SW480 shCYP1B1 cells. Obvious reductions of several LCFAs such as C20:1, C20:3, or C20:5 was observed in SW480 shCYP1B1 cells (*Figure 6A,6B*). Next, we examined whether these LCFAs could reverse the suppressive effects of *CYP1B1* knockdown on cell growth in SW480 shCYP1B1 cells. The results showed that C20:1 and C20:3 enhanced the cell growth of SW480 shCYP1B1 cells *in vitro* (*Figure 6C*), and increased tumor growth *in vivo* (Figure S6A). Interestingly, C20:0 also exhibited pro-growth effect in SW480 shCYP1B1 cells, probably because it can be further metabolized to C20:1 and C20:3 (22). Finally, we examined the effects of these LCFAs on the expression of *CYP1B1*-regulated genes involved in G1/S transition, and found that C20:3 could significantly upregulate the expression of *MCM5*, *PCNA*, and *FEN1* in SW480 shCYP1B1 cells (*Figure 6D* and Figure S6B-S6D). C20:0 and C20:1 treatment also led to moderate increase of expression of *MCM5*, *PCNA*, and *FEN1* (*Figure 6D* and Figure S6B-S6D). Similar results were observed *in vitro* and *in vivo* by using HT29 shCYP1B1 cells (*Figure 6E,6F* and Figure S6E-S6H). These results support the notion that specific LCFAs induced by *CYP1B1* promote metastatic CRC cell growth by up-regulating the expression of *MCM5*, *PCNA*, and *FEN1*.

Discussion

In this study, we identified *CYP1B1*-mediated fatty acids metabolic alteration as a key pathway for the outgrowth of metastatic CRC cells in the liver. A previous study showed

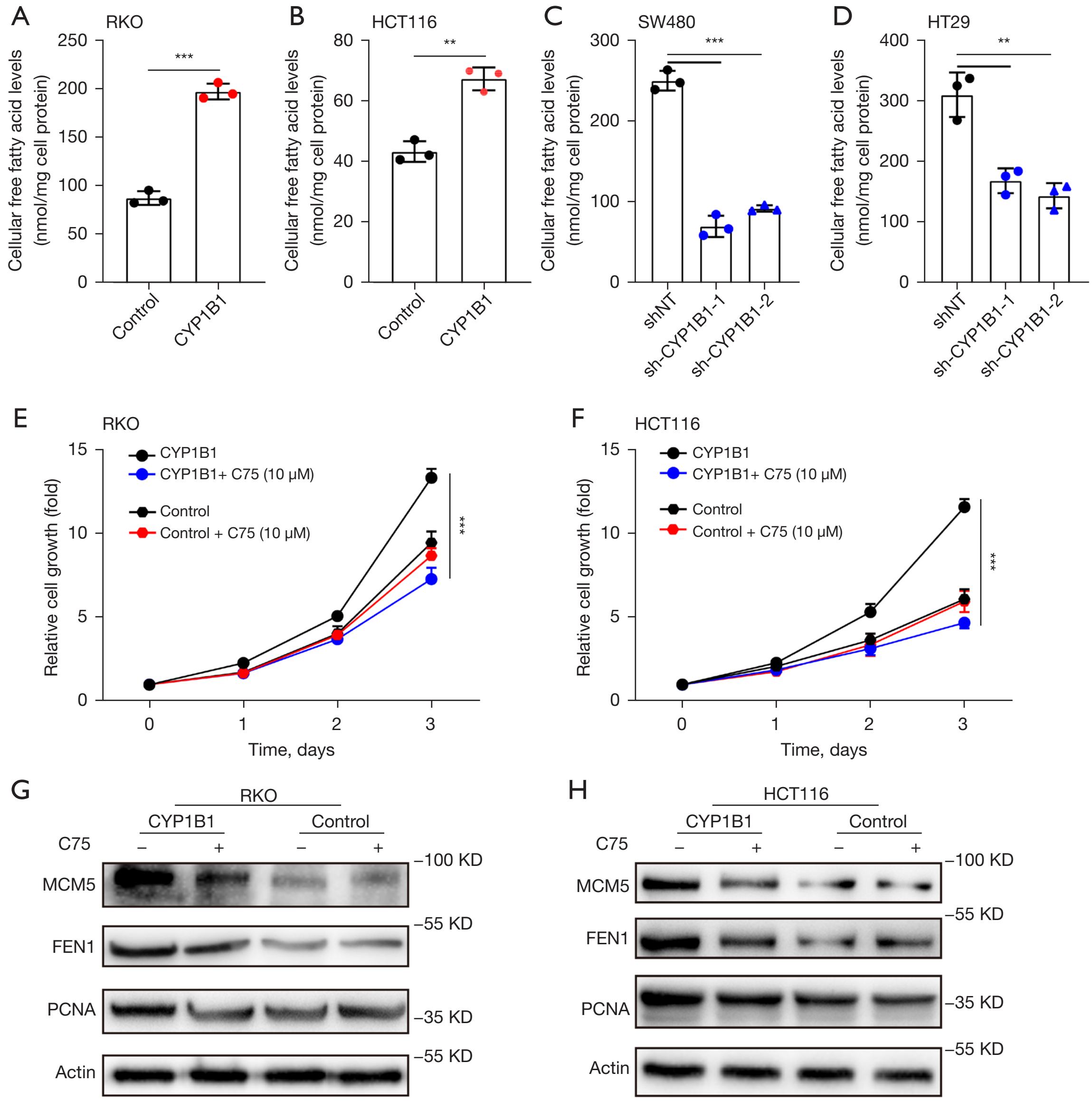

Figure 5 *CYP1B1* promotes CRC cell growth by enhancing fatty acids biosynthesis. (A-D) The effects of manipulating *CYP1B1* on cellular FFAs levels in CRC cells. (E,F) Inhibition of fatty acid biosynthesis suppresses the pro-tumor effect of *CYP1B1* in CRC cells. The effect of C75 (10 μM) treatment on cell growth in *CYP1B1* overexpressed RKO cells and HCT116 cells. The relative cell number is expressed as fold change to day 0. (G,H) C75 suppresses growth-related genes expression in CRC cells. The protein levels of *MCM5*, *FEN1*, and *PCNA* in RKO and HCT116 groups were decreased after C75 (10 μM) intervention for 48 hours. Data are shown as mean ± SD of triplicate or quinary experiments (A-D and E,F). Significance was determined by Student's *t*-test (A,B), one-way ANOVA (C,D) or two-way ANOVA (E,F). **, P<0.01; ***, P<0.001. shNT, non-target shRNA control; CRC, colorectal cancer; FFAs, free fatty acids; SD, standard deviation; ANOVA, analysis of variance.

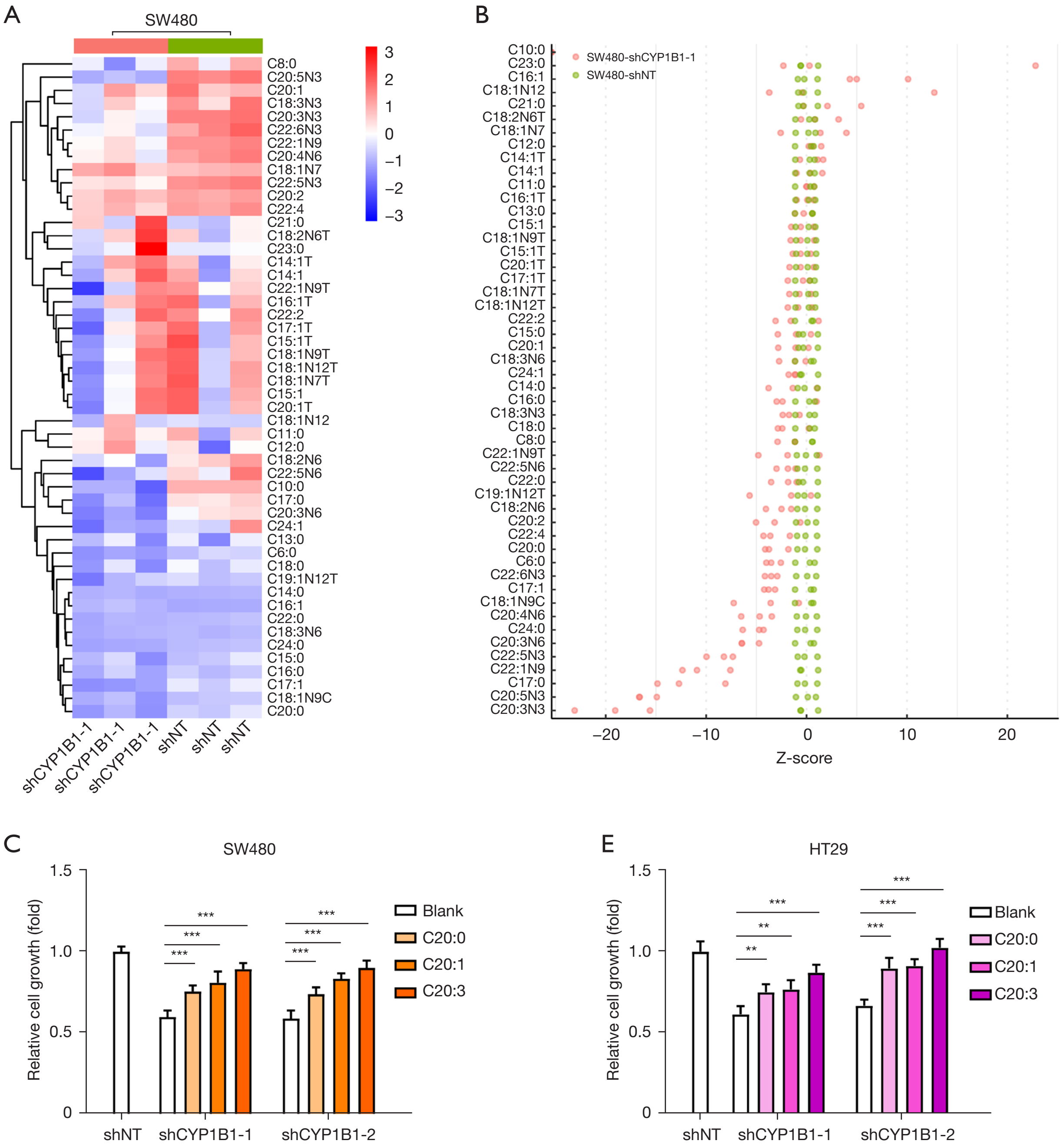
A
SW480
C8:0
C20:5N3
C20:1
C18:3N3
C20:3N3
C22:6N3
C22:1N9
C20:4N6
C18:1N7
C22:5N3
C20:2
C22:4
C21:0
C18:2N6T
C23:0
C14:1T
C14:1
C22:1N9T
C16:1T
C22:2
C17:1T
C15:1T
C18:1N9T
C18:1N12T
C18:1N7T
C15:1
C20:1T
C18:1N12
C11:0
C12:0
C18:2N6
C22:5N6
C10:0
C17:0
C20:3N6
C24:1
C13:0
C6:0
C18:0
C19:1N12T
C14:0
C16:1
C22:0
C18:3N6
C24:0
C15:0
C16:0
C17:1
C18:1N9C
C20:0
3
2
1
0
−1
−2
−3
shCYP1B1-1
shCYP1B1-1
shCYP1B1-1
shNT
shNT
shNT
B
SW480-shCYP1B1-1
SW480-shNT
C10:0
C23:0
C16:1
C18:1N12
C21:0
C18:2N6T
C18:1N7
C12:0
C14:1T
C14:1
C11:0
C16:1T
C13:0
C15:1
C18:1N9T
C15:1T
C20:1T
C17:1T
C18:1N7T
C18:1N12T
C22:2
C15:0
C20:1
C18:3N6
C24:1
C14:0
C16:0
C18:3N3
C18:0
C8:0
C22:1N9T
C22:5N6
C22:0
C19:1N12T
C18:2N6
C20:2
C22:4
C20:0
C6:0
C22:6N3
C17:1
C18:1N9C
C20:4N6
C24:0
C20:3N6
C22:5N3
C22:1N9
C17:0
C20:5N3
C20:3N3
−20
−10
0
10
20
Z-score
C
SW480
Relative cell growth (fold)
1.5
1.0
0.5
0
***
***
***
***
***
***
Blank
C20:0
C20:1
C20:3
shNT
shCYP1B1-1
shCYP1B1-2
E
HT29
Relative cell growth (fold)
1.5
1.0
0.5
0
***
**
**
***
***
***
Blank
C20:0
C20:1
C20:3
shNT
shCYP1B1-1
shCYP1B1-2

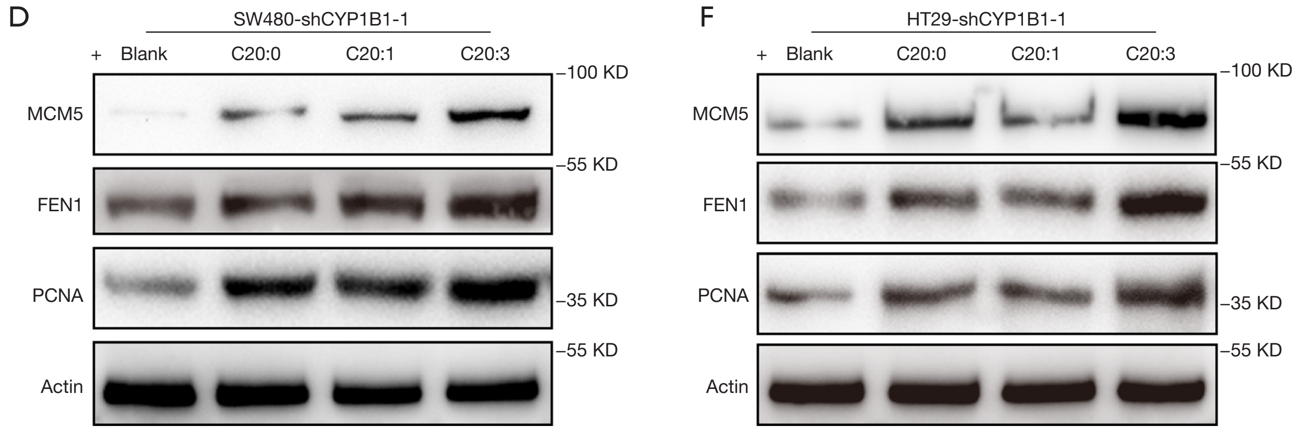

Figure 6 LCFAs up-regulate the expression of *MCM5*, *PCNA*, and *FEN1*. (A,B) The effects of manipulating *CYP1B1* on cellular LCFA levels. Cellular LCFAs levels in SW480 shNT and SW480 shCYP1B1 cells were determined by GC-MS. The top differential LCFAs altered in SW480 shCYP1B1 cells are shown in (A), and Z-score plot of these metabolites are shown in (B). Each point represents one metabolite in one sample. (C) LCFAs promote cell proliferation of SW480 shCYP1B1 cells *in vitro*. The effects of 3 LCFAs (20:0, 20:1, 20:3; 50 μM) on cell proliferation of SW480 shCYP1B1 cells. Data are shown as mean ± SD of quinary experiments, and the relative cell number of control cells is expressed as 1. Significance was determined by one-way ANOVA. (D) The effect of LCFAs on the expression of *MCM5*, *PCNA*, and *FEN1* in SW480 shCYP1B1 cells. After treatment with LCFAs (50 μM) for 48 hours, protein levels of *MCM5*, *PCNA*, and *FEN1* were determined by western blotting. (E) LCFAs promote cell proliferation of HT29 shCYP1B1 cells *in vitro*. The effects of 3 LCFAs (20:0, 20:1, 20:3; 50 μM) on cell proliferation of HT29 shCYP1B1 cells. Data are shown as mean ± SD of quinary experiments, and the relative cell number of control cells is expressed as 1. Significance was determined by one-way ANOVA. (F) The effect of LCFAs on the expression of *MCM5*, *PCNA*, and *FEN1* in HT29 shCYP1B1 cells. After treatment with LCFAs (50 μM) for 48 hours, protein levels of *MCM5*, *PCNA*, and *FEN1* were determined by western blotting. **, P<0.01; ***, P<0.001. shNT, non-target shRNA control; LCFA, long chain fatty acid; GC-MS, gas chromatography mass spectrometry; SD, standard deviation; ANOVA, analysis of variance.

that *Cyp1b1* disruption altered the expression of a large number of liver-specific genes in an animal study (23), suggesting that *CYP1B1* plays an important role in the liver. A recent study has shown that liver metastatic CRC cells gain a liver-specific gene transcription program, while losing their colon-specific gene transcription program (24). Our results also support this conclusion.

CYP1B1 is a member of the cytochrome P450 enzyme family 1, and is also shown to be important in regulating many metabolic pathways, including the metabolism of fatty acids, steroid hormones, vitamins, and melatonin (25). *CYP1B1* is also reported to be highly expressed in various cancers such as prostate, breast, and colon cancer (12,13,26), and *CYP1B1*-mediated carcinogenesis may depend on its enzymatic activity (27). Although one previous study showed *CYP1B1* is highly expressed in patients with distant metastasis of COAD, its specific role remains unclear (15). Our work revealed that *CYP1B1* facilitates G1/S transition of CRC cells via regulating fatty acid metabolism. Further studies are needed to determine whether other *CYP1B1*-regulated metabolic pathways also contribute to the pro-growth effect of *CYP1B1* in CRC cells.

The mechanism underlying the upregulation of *CYP1B1* in LM of CRC is still undetermined. Hwang *et al.* reported that peroxisome proliferator-activated receptor α (PPARα) agonist increased *CYP1B1* expression in breast cancer cells (28). Another study using CRC found that interleukin-6 promoted the nuclear translocation of DNMT1, and reduced miR-27b expression by interacting with CpG island region of miR-27b, resulting in the increase of *CYP1B1* mRNA level (14). Meanwhile, most researchers focus on effects of *CYP1B1* on estrogen, and have concentrated on estrogen-related tumors (12,29). In fact, one of the functions of *CYP1B1* is participating in fatty acid metabolism. For example, *CYP1B1* catalyzes the formation of hydroxy eicosatetraenoic acid from arachidonic acid (30), the latter having been shown to promote lung adenocarcinoma cells proliferation and migration by activating the STAT3 phosphorylation signaling pathway (31).

FFAs are closely associated with cancer progression. One early case-control study found that an increased incidence of CRC was associated with the consumption of saturated fatty acids (SFAs)-rich foods (32). In a mouse study investigating the relationship between inflammation and tumors through the knockout of intestinal epithelial SCD1, researchers found that the loss of SCD1 led to an increase in SFAs (stearic and palmitic acids) compared to unsaturated fatty acids (UFAs; oleic and palmitoleic acids), which promoted the progression of intestinal inflammation and subsequent tumor occurrence (33). Interestingly, some increases in SFAs can be beneficial. An early study reported that SFAs, particularly medium-chain SFAs such as capric, caprylic, and caproic acids, significantly inhibited the growth of human colon, skin, and breast cancers by downregulating cell cycle genes and upregulating apoptosis-related genes (34).

In our study, LCFAs treatment led to the elevated expression of cell cycle-regulating genes such as *MCM5* (*Figure 6E,6F*). The expression of MCM family proteins can only be detected during the cell proliferation period. Its expression reaches a peak at the G1/S transition point and is absent in the M and G0 phases. Therefore, it can serve as a specific marker for cell proliferation (35). The MCM family contains several members including *MCM2* to *MCM7*, which are mainly involved in the formation of replication forks and recruitment of other DNA replication-related proteins (36,37). We found that manipulating *CYP1B1* only affected *MCM5* expression and no other members of MCM family (*Figure 4C* and Figure S4). Literature suggests that although members of the MCM family possess helicase activity, their contribution values differ among subunits, which are related to the adenosine triphosphate (ATP)-binding sites (38). As we know, *CYP1B1* itself is a cytochrome P450 monooxygenase that can transfer electrons with NADPH through redox reactions (39), and the relationship between NADPH and ATP is well known. Therefore, it is possible that *CYP1B1* affects *MCM5* by affecting the ATP site activity on its structural domain, resulting in changes in the proliferative phenotype. Meanwhile, regarding FFA promoting proliferation, some articles have indicated that FFA can mediate the release of reactive oxygen species (ROS) during mitochondrial oxidative metabolism, which promotes smooth muscle cell proliferation (40). In a biochemical redox reaction, a study showed that the electrophilic activity of fatty acid nitroalkenes can react rapidly and reversibly with cysteine, regulating inflammation and cell proliferation in the microenvironment (41). A recent article also explicitly states that the effects of FFA on multiple myeloma (MM) cells differ depending on the dosage: low doses promote MM proliferation through the ROS system, whereas high doses exhibit lipotoxicity through the iron death pathway, inhibiting their proliferation (42). We know that lipid oxidation, ROS metabolism, and mitochondrial function are closely related to the endoplasmic reticulum and mitochondria. Mitochondria are also important organelles for ATP production, as we have already discussed that the ATP binding site is present in the chemical structure of the MCM2-7 protein family. Therefore, our hypothesis is that LCFAs change the ATP site to mediate changes in proliferation-related genes such as *MCM5*. Certainly, our research has some flaws. One limitation is that we failed to monitor NSG with imaging equipment during the whole period and only measured liver weight with an electronic balance, ignoring the collection of bloods from animals, leading to imperfection of animal experiments. Another flaw is that we did not expose the specific mechanism about upstream regulation of *CYP1B1* in liver. Our current preliminary experiments hint that the expression of *CYP1B1* is closely related to the liver immune microenvironment (data are not shown), which will be further testified in future studies.

Conclusions

In summary, our study has demonstrated that regulation of *CYP1B1* in CRC cells could affect downstream proliferation-related factors such as *MCM5* via LCFAs, leading to an impact on tumor cell growth and promoting malignant progression of CRC LM. As "CYP1B1-LCFAs-G1/S transition" may be significant mechanisms for progression of CRC LM, perturbing fatty acid synthesis opens a new revenue for treatment of LM, especially targeting "CYP1B1-LCFAs", which will become a new method (*Figure 7*).

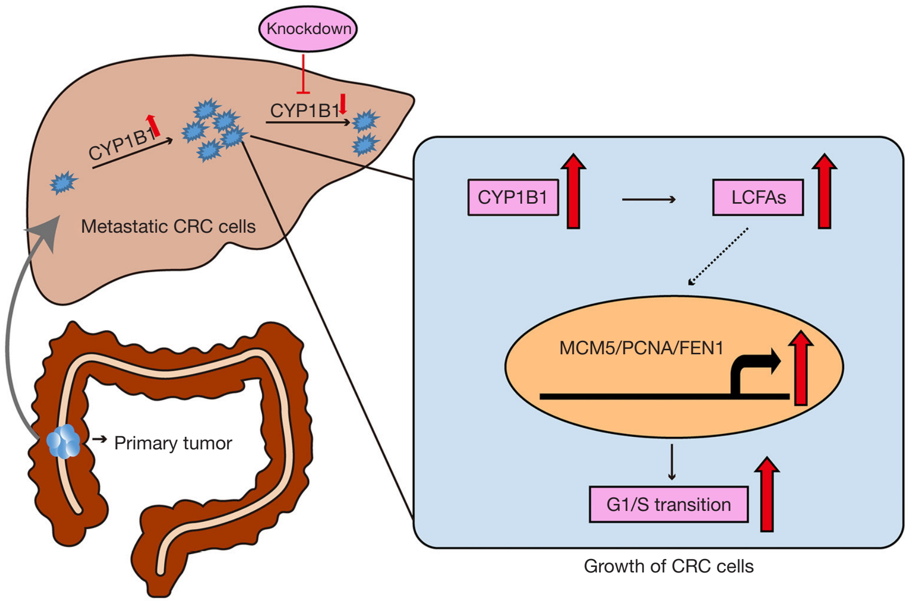

Figure 7 Schematic illustration depicting the roles of *CYP1B1* in promoting liver metastases of CRC. CYP1B1 is highly expressed in liver metastases of CRC. *CYP1B1* promotes CRC liver metastasis by enhancing CRC cell proliferation (MCM5/PCNA/FEN1 axis activation) in a fatty acid-dependent way. Final proliferation phenotype is achieved via G1/S transition enhancement. CRC, colorectal cancer; LCFA, long chain fatty acid.

Acknowledgments

Funding: This work was funded by the National Nature Science Foundation of China (Nos. 81972737, 82172739, 82272774, and 82072666).

Footnote

Reporting Checklist: The authors have completed the ARRIVE reporting checklist. Available at https://jgo.amegroups.com/article/view/10.21037/jgo-23-895/rc

Data Sharing Statement: Available at https://jgo.amegroups.com/article/view/10.21037/jgo-23-895/dss

Peer Review File: Available at https://jgo.amegroups.com/article/view/10.21037/jgo-23-895/prf

Conflicts of Interest: All authors have completed the ICMJE uniform disclosure form (available at https://jgo.amegroups.com/article/view/10.21037/jgo-23-895/coif). The authors have no conflicts of interest to declare.

Ethical Statement: The authors are accountable for all aspects of the work in ensuring that questions related to the accuracy or integrity of any part of the work are appropriately investigated and resolved. Animal experiments were treated in strict accordance with animal care procedures and methods approved by Institutional Animal Care and Use Committee at Shanghai Institute of Nutrition and Health, Chinese Academy of Sciences (No. SINH-2022-LM-1). Experiments were in compliance with Chinese National Standard (GBT35823-2018) for the care and use of animals. For human research, the study was conducted in accordance with the Declaration of Helsinki (as revised in 2013). This study was performed based on ethical standards of Institutional Review Board in Zhongshan Hospital of Fudan University (No. B2020-348R), China. Informed consent was taken from all the patients.

References

1. Massagué J, Obenauf AC. Metastatic colonization by circulating tumour cells. Nature 2016;529:298-306.
2. Hanahan D, Weinberg RA. Hallmarks of cancer: the next generation. Cell 2011;144:646-74.
3. Schild T, Low V, Blenis J, et al. Unique Metabolic Adaptations Dictate Distal Organ-Specific Metastatic Colonization. Cancer Cell 2018;33:347-54.
4. Lee JK, Merchant SA, Jensen CD, et al. Rising Early-onset Colorectal Cancer Incidence Is Not an Artifact of Increased Screening Colonoscopy Use in a Large, Diverse Healthcare System. Gastroenterology 2022;162:325-327.e3.
5. Hess KR, Varadhachary GR, Taylor SH, et al. Metastatic patterns in adenocarcinoma. Cancer 2006;106:1624-33.
6. Nordlinger B, Sorbye H, Glimelius B, et al. Perioperative FOLFOX4 chemotherapy and surgery versus surgery alone for resectable liver metastases from colorectal cancer (EORTC 40983): long-term results of a randomised, controlled, phase 3 trial. Lancet Oncol 2013;14:1208-15.
7. Cloyd JM, Mizuno T, Kawaguchi Y, et al. Comprehensive Complication Index Validates Improved Outcomes Over Time Despite Increased Complexity in 3707 Consecutive Hepatectomies. Ann Surg 2020;271:724-31.
8. Badawi AF, Cavalieri EL, Rogan EG. Role of human cytochrome P450 1A1, 1A2, 1B1, and 3A4 in the 2-, 4-, and 16alpha-hydroxylation of 17beta-estradiol. Metabolism 2001;50:1001-3.
9. Belous AR, Hachey DL, Dawling S, et al. Cytochrome P450 1B1-mediated estrogen metabolism results in estrogen-deoxyribonucleoside adduct formation. Cancer Res 2007;67:812-7.
10. Yaghini FA, Song CY, Lavrentyev EN, et al. Angiotensin II-induced vascular smooth muscle cell migration and growth are mediated by cytochrome P450 1B1-dependent superoxide generation. Hypertension 2010;55:1461-7.
11. Christou M, Savas U, Schroeder S, et al. Cytochromes CYP1A1 and CYP1B1 in the rat mammary gland: cell-specific expression and regulation by polycyclic aromatic hydrocarbons and hormones. Mol Cell Endocrinol 1995;115:41-50.
12. Mohamed HT, Gadalla R, El-Husseiny N, et al. Inflammatory breast cancer: Activation of the aryl hydrocarbon receptor and its target CYP1B1 correlates closely with Wnt5a/b-beta-catenin signalling, the stem cell phenotype and disease progression. J Adv Res 2018;16:75-86.
13. Lin Q, Cao J, Du X, et al. CYP1B1-catalyzed 4-OHE2 promotes the castration resistance of prostate cancer stem cells by estrogen receptor alpha-mediated IL6 activation. Cell Commun Signal 2022;20:31.
14. Patel SA, Bhambra U, Charalambous MP, et al. Interleukin-6 mediated upregulation of CYP1B1 and CYP2E1 in colorectal cancer involves DNA methylation, miR27b and STAT3. Br J Cancer 2014;111:2287-96.
15. Gu L, Liu Y, Jiang C, et al. Identification and clinical validation of metastasis-associated biomarkers based on large-scale samples in colon-adenocarcinoma. Pharmacol Res 2020;160:105087.
16. Chen S, Zhou Y, Chen Y, et al. fastp: an ultra-fast all-in-one FASTQ preprocessor. Bioinformatics 2018;34:i884-90.
17. Kim D, Langmead B, Salzberg SL. HISAT: a fast spliced aligner with low memory requirements. Nat Methods 2015;12:357-60.
18. Anders S, Pyl PT, Huber W. HTSeq--a Python framework to work with high-throughput sequencing data. Bioinformatics 2015;31:166-9.
19. Love MI, Huber W, Anders S. Moderated estimation of fold change and dispersion for RNA-seq data with DESeq2. Genome Biol 2014;15:550.
20. Hoving LR, Heijink M, van Harmelen V, et al. GC-MS Analysis of Medium- and Long-Chain Fatty Acids in Blood Samples. Methods Mol Biol 2018;1730:257-65.
21. Beccaria M, Franchina FA, Nasir M, et al. Investigation of mycobacteria fatty acid profile using different ionization energies in GC-MS. Anal Bioanal Chem 2018;410:7987-96.
22. Dyall SC, Balas L, Bazan NG, et al. Polyunsaturated fatty acids and fatty acid-derived lipid mediators: Recent advances in the understanding of their biosynthesis, structures, and functions. Prog Lipid Res 2022;86:101165.
23. Larsen MC, Bushkofsky JR, Gorman T, et al. Cytochrome P450 1B1: An unexpected modulator of liver fatty acid homeostasis. Arch Biochem Biophys 2015;571:21-39.
24. Teng S, Li YE, Yang M, et al. Tissue-specific transcription reprogramming promotes liver metastasis of colorectal cancer. Cell Res 2020;30:34-49.
25. Shah BR, Xu W, Mraz J. Cytochrome P450 1B1: role in health and disease and effect of nutrition on its expression. RSC Adv 2019;9:21050-62.
26. Meng Q, Wang Z, Cui J, et al. Design, Synthesis, and Biological Evaluation of Cytochrome P450 1B1 Targeted Molecular Imaging Probes for Colorectal Tumor

Detection. J Med Chem 2018;61:10901-9.
27. Kwon YJ, Baek HS, Ye DJ, et al. CYP1B1 Enhances Cell Proliferation and Metastasis through Induction of EMT and Activation of Wnt/beta-Catenin Signaling via Sp1 Upregulation. PLoS One 2016;11:e0151598.
28. Hwang YP, Won SS, Jin SW, et al. WY-14643 Regulates CYP1B1 Expression through Peroxisome Proliferator-Activated Receptor alpha-Mediated Signaling in Human Breast Cancer Cells. Int J Mol Sci 2019;20:5928.
29. Malik DE, David RM, Gooderham NJ. Interleukin-6 selectively induces drug metabolism to potentiate the genotoxicity of dietary carcinogens in mammary cells. Arch Toxicol 2019;93:3005-20.
30. Elbekai RH, El-Kadi AO. Cytochrome P450 enzymes: central players in cardiovascular health and disease. Pharmacol Ther 2006;112:564-87.
31. Yang L, Ma C, Zhang L, et al. 15-Lipoxygenase-2/15(S)-hydroxyeicosatetraenoic acid regulates cell proliferation and metastasis via the STAT3 pathway in lung adenocarcinoma. Prostaglandins Other Lipid Mediat 2018;138:31-40.
32. Chun YJ, Sohn SK, Song HK, et al. Associations of colorectal cancer incidence with nutrient and food group intakes in korean adults: a case-control study. Clin Nutr Res 2015;4:110-23.
33. Ducheix S, Peres C, Härdfeldt J, et al. Deletion of Stearoyl-CoA Desaturase-1 From the Intestinal Epithelium Promotes Inflammation and Tumorigenesis, Reversed by Dietary Oleate. Gastroenterology 2018;155:1524-1538.e9.
34. Narayanan A, Baskaran SA, Amalaradjou MA, et al. Anticarcinogenic properties of medium chain fatty acids on human colorectal, skin and breast cancer cells in vitro. Int J Mol Sci 2015;16:5014-27.
35. Baris Y, Taylor MRG, Aria V, et al. Fast and efficient DNA replication with purified human proteins. Nature 2022;606:204-10.
36. Jones ML, Baris Y, Taylor MRG, et al. Structure of a human replisome shows the organisation and interactions of a DNA replication machine. EMBO J 2021;40:e108819.
37. Jenkyn-Bedford M, Jones ML, Baris Y, et al. A conserved mechanism for regulating replisome disassembly in eukaryotes. Nature 2021;600:743-7.
38. Rzechorzek NJ, Hardwick SW, Jatikusumo VA, et al. CryoEM structures of human CMG-ATPgammaS-DNA and CMG-AND-1 complexes. Nucleic Acids Res 2020;48:6980-95.
39. Lee AJ, Cai MX, Thomas PE, et al. Characterization of the oxidative metabolites of 17beta-estradiol and estrone formed by 15 selectively expressed human cytochrome p450 isoforms. Endocrinology 2003;144:3382-98.
40. Stockwell BR, Friedmann Angeli JP, Bayir H, et al. Ferroptosis: A Regulated Cell Death Nexus Linking Metabolism, Redox Biology, and Disease. Cell 2017;171:273-85.
41. Grippo V, Mojovic M, Pavicevic A, et al. Electrophilic characteristics and aqueous behavior of fatty acid nitroalkenes. Redox Biol 2021;38:101756.
42. Yao Y, Sun S, Wang J, et al. Canonical Wnt Signaling Remodels Lipid Metabolism in Zebrafish Hepatocytes following Ras Oncogenic Insult. Cancer Res 2018;78:5548-60.

Cite this article as: Jin L, Huang J, Guo L, Zhang B, Li Q, Li H, Yu M, Xie P, Yu Q, Chen Z, Liu S, Xu Y, Xiao Y, Lu M, Ye Q. *CYP1B1* promotes colorectal cancer liver metastasis by enhancing the growth of metastatic cancer cells via a fatty acids-dependent manner. J Gastrointest Oncol 2023;14(6):2448-2465. doi: 10.21037/jgo-23-895

Supplementary

Table S1 Primers for quantitative RT-PCR

Primer	Sequence
CYP1B1-forward	5'-GGCTGGATTTGGAGAACGTA-3'
CYP1B1-reverse	5'-CATAAAGGAAGGCCAGGACA-3'
GAPDH-forward	5'-ACCCACTCCTCCACCTTTG-3'
GAPDH-reverse	5'-CTGTAGCCAAATTCGTTGTCAT-3'
MCM2-forward	5'-ACCAGGACAGAACCAGCATC-3'
MCM2-reverse	5'-CAGGATGTCAAAGCGTGAGA-3'
MCM3-forward	5'-TGTGGAGGGCATTGTCACTA-3'
MCM3-reverse	5'-CAAGGGGATTGTTCTCCTCA-3'
MCM5-forward	5'-CTGGGGGAGTACTGGATTGA-3'
MCM5-reverse	5'-ATGACCTGGATGTCCTGGAG-3'
PCNA-forward	5'-CGGATACCTTGGCGCTAGTA-3'
PCNA-reverse	5'-TCACTCCGTCTTTTGCACAG-3'
FEN1-forward	5'-GACATGGACTGCCTCACCTT-3'
FEN1-reverse	5'-CCCAATACCCCGGATACTCT-3'
LIG1-forward	5'-AGGAGTGGAATGGAGTGGTG-3'
LIG1-reverse	5'-AGGTGTCAGAGAGGGAAGCA-3'
Actin-forward	5'-GGACTTCGAGCAAGAGATGG-3'
Actin-reverse	5'-AGCACTGTGTTGGCGTACAG-3'

RT-PCR, real-time polymerase chain reaction.

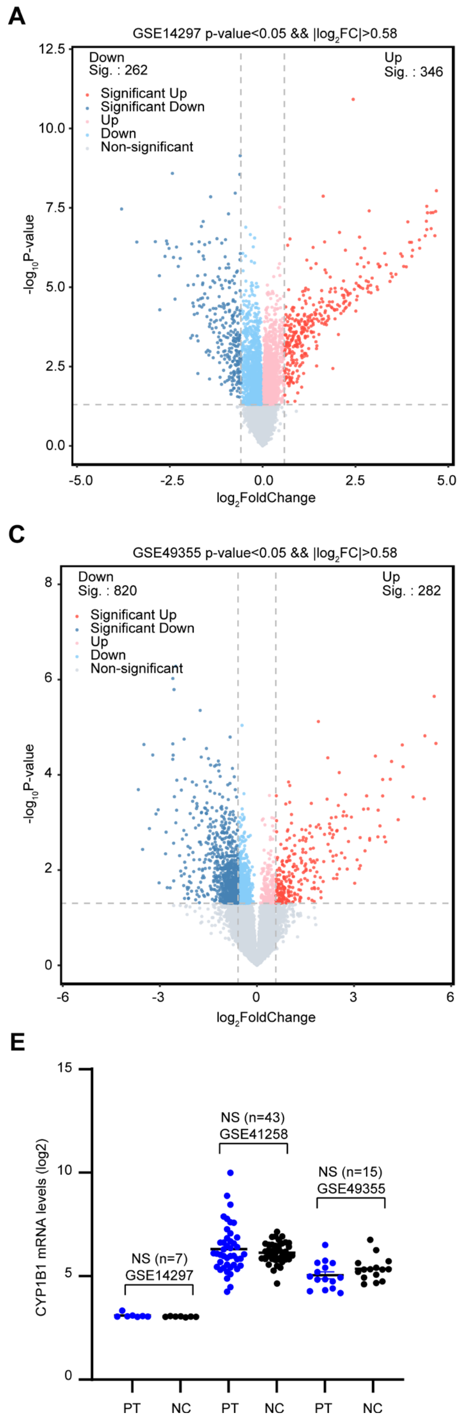

Figure S1 Genes between LM and PT from four GSE databases and CYP1B1 mRNA levels in PT and normal colon tissues (NC) from three GSE databases. (A-D) Volcano plot of mRNA profiles from 4 GSE databases. 346 up-regulated genes and 262 down-regulated genes are shown in (A) (n=18). 198 up-regulated genes and 63 down-regulated genes are shown in (B) (n=5) (B). 282 up-regulated genes and 820 down-regulated genes are shown in (C) (n=13). 500 up-regulated genes and 312 down-regulated genes are shown in (D) (n=7). (E) The CYP1B1 mRNA levels in PT and NC from three GSE databases. Each dot represents the relative mRNA level in PT or NC in each tissue sample from 3 GSE databases, data are shown as mean ± SEM. Significance was determined by a 2-tailed paired *t*-test. NS, not significant as indicated. LM, liver metastases; PT, primary tumors; GSE, GEO series; mRNA, messenger RNA; SEM, standard error of the mean.

 https://dx.doi.org/10.21037/jgo-23-895

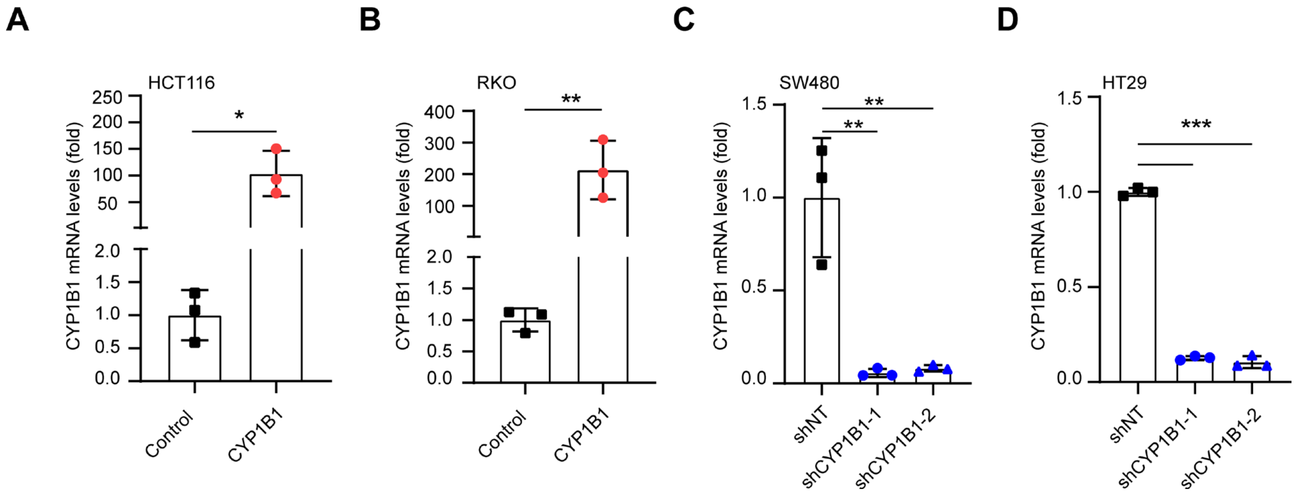

Figure S2 Confirmation of *CYP1B1* overexpression and knockdown in CRC cell lines. (A-D) Quantitative RT-PCR confirms *CYP1B1* overexpression and knockdown in CRC cell lines. The *CYP1B1* mRNA levels increased by about 100-fold in HCT116 (A) and 200-fold in RKO (B), decreased by about 80–90% in SW480 or HT29 (C,D). Representative results from at least three independent experiments are shown. Data are shown as mean ± SD. Significance was determined by Student's *t*-test (A,B) or one-way ANOVA (C,D). *, $P<0.05$; **, $P<0.01$; ***, $P<0.001$. shNT, non-target shRNA control; CRC, colorectal cancer; RT-PCR, real-time polymerase chain reaction; mRNA, messenger RNA; SD, standard deviation; ANOVA, analysis of variance.

 https://dx.doi.org/10.21037/jgo-23-895

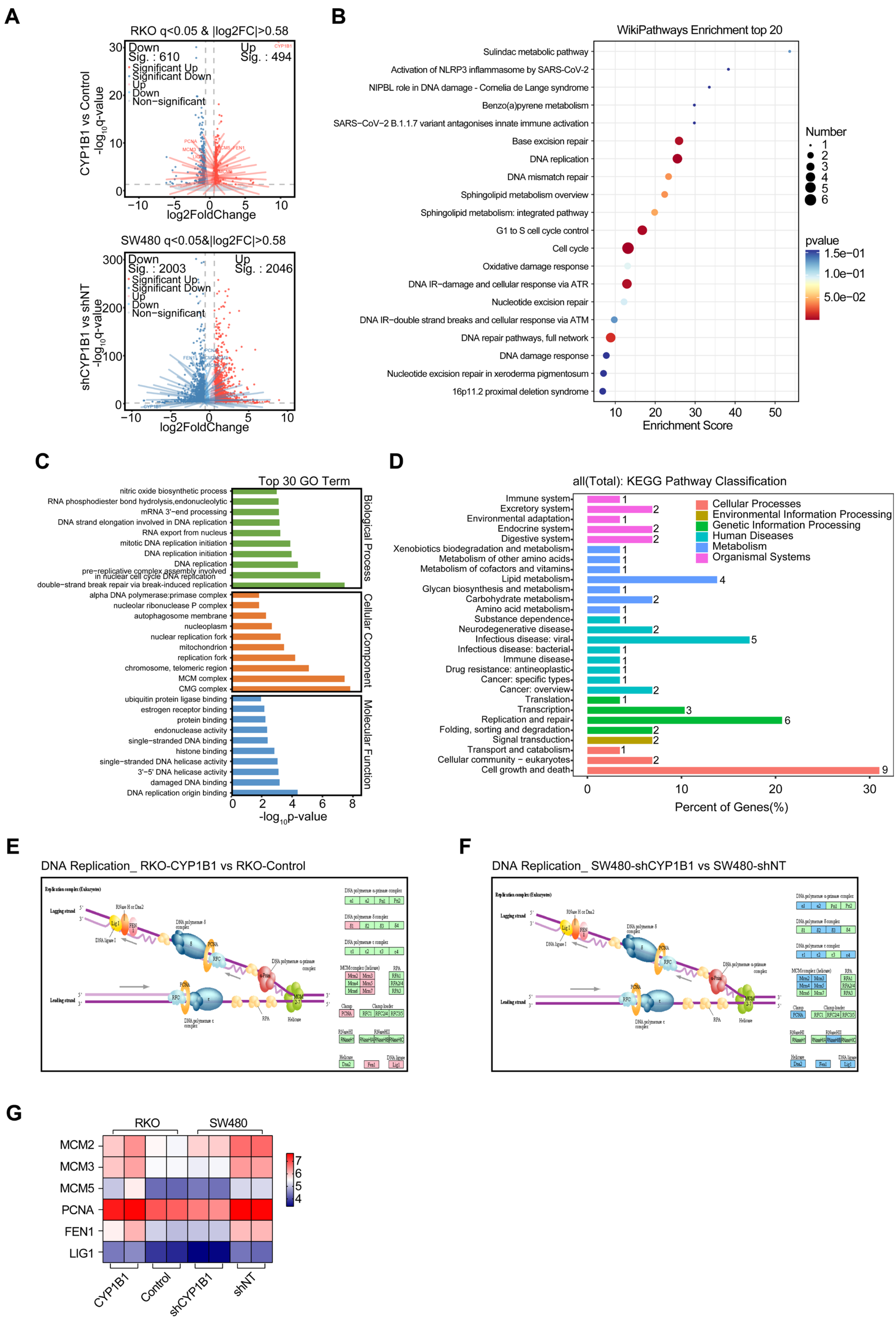

Figure S3 Enrichment analysis of potential *CYP1B1*-regulated genes. (A) Volcano plot of mRNA profiles from overexpression and knockdown cell groups. 494 up-regulated genes and 610 down-regulated genes in RKO group are shown in CYP1B1 VS control. 2,046 up-regulated genes and 2,003 down-regulated genes in SW480 group are shown in Graph shCYP1B1 VS shNT. (B-D) Enrichments of 59 genes between RKO up-regulated genes and SW480 down-regulated genes. WikiPathways enrichment shows 59 genes are mainly concentrated in cell cycle, DNA replication, etc. (B). GO analysis shows 59 genes were mainly concentrated in MCM complex, DNA replication origin binding, etc. (C). KEGG Pathway shows 59 genes are mainly concentrated in cell growth and death, replication and repair, etc. (D). (E,F) DNA replication diagram in RKO and SW480. MCM2, MCM3, MCM5, etc. are up-regulated in the DNA replication diagram of RKO group (E). FEN1, LIG1, DNA2, etc. are down-regulated in the DNA replication diagram of SW480 group (F). (G) Six growth-related differential genes from overexpression and knockdown cell groups. Data are shown in heat map with logarithm of two. GO, Gene Ontology; KEGG, Kyoto Encyclopedia of Genes and Genomes; shNT, non-target shRNA control; mRNA, messenger RNA.

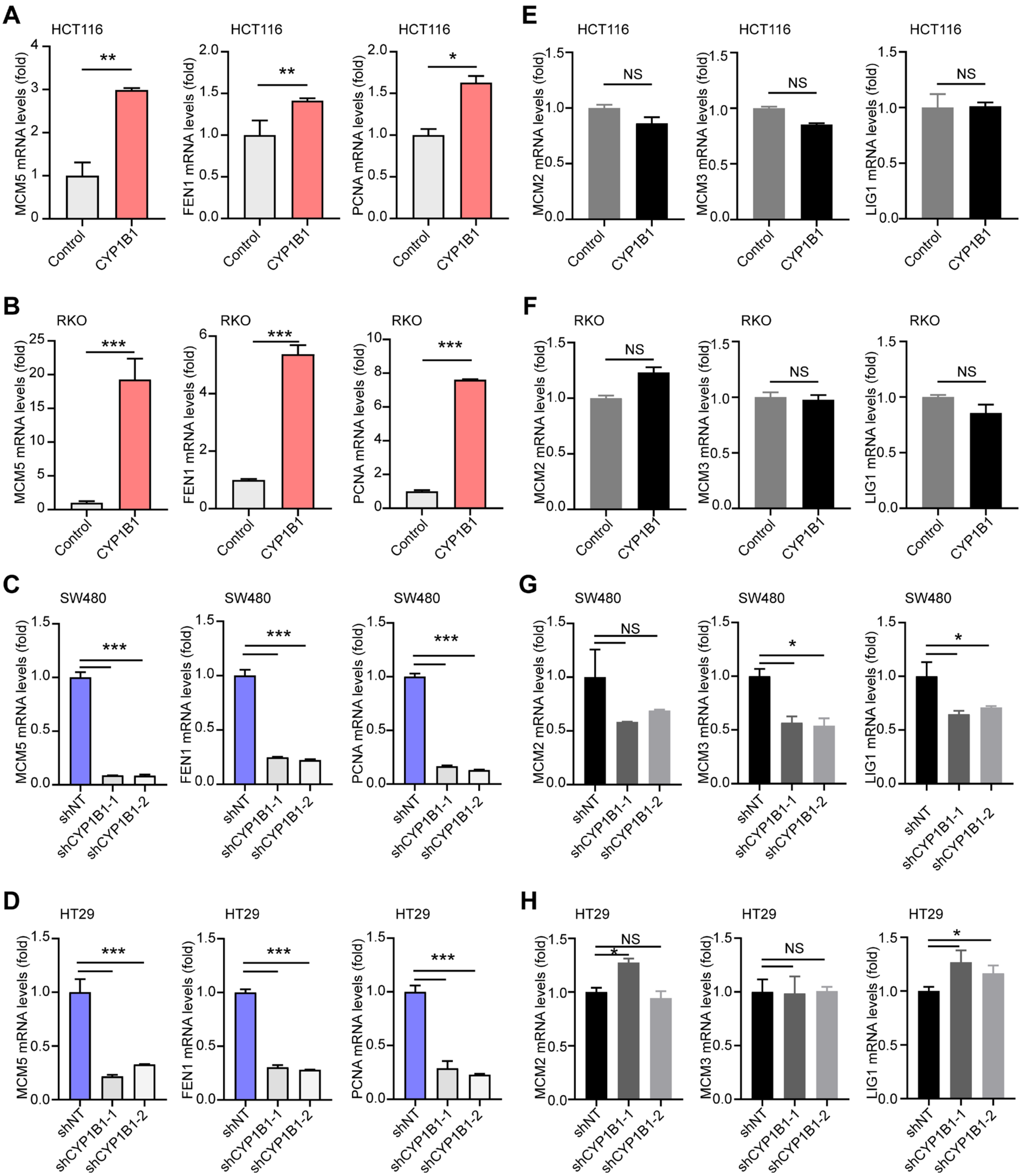

Figure S4 *CYP1B1* regulates CRC cell growth by regulating expressions of *MCM5*, *PCNA*, and *FEN1*. (A-D) Positive genes challenge were verified in CRC cell lines by quantitative RT-PCR. The mRNA levels of MCM5, FEN1 and PCNA are up-regulated after CYP1B1 overexpression in HCT116 and RKO (A,B). The mRNA levels of *MCM5*, *FEN1*, and *PCNA* are down-regulated after *CYP1B1* knockdown in SW480 and HT29 (C,D). (E-H) Negative genes challenge were verified in CRC cell lines by quantitative RT-PCR. *MCM2*, *MCM3*, or *LIG1* show unrelated tendency in CRC cells after *CYP1B1* intervention (E-H). Representative results from at least 3 independent experiments are shown. Data are shown as mean ± SD. Significance was determined by Student's *t*-test (A,B,E,F) or one-way ANOVA (C,D,G,H). *, P<0.05; **, P<0.01; ***, P<0.001. NS, not significant as indicated. shNT, non-target shRNA control; CRC, colorectal cancer; RT-PCR, real-time polymerase chain reaction; mRNA, messenger RNA; SD, standard deviation; ANOVA, analysis of variance.

 https://dx.doi.org/10.21037/jgo-23-895

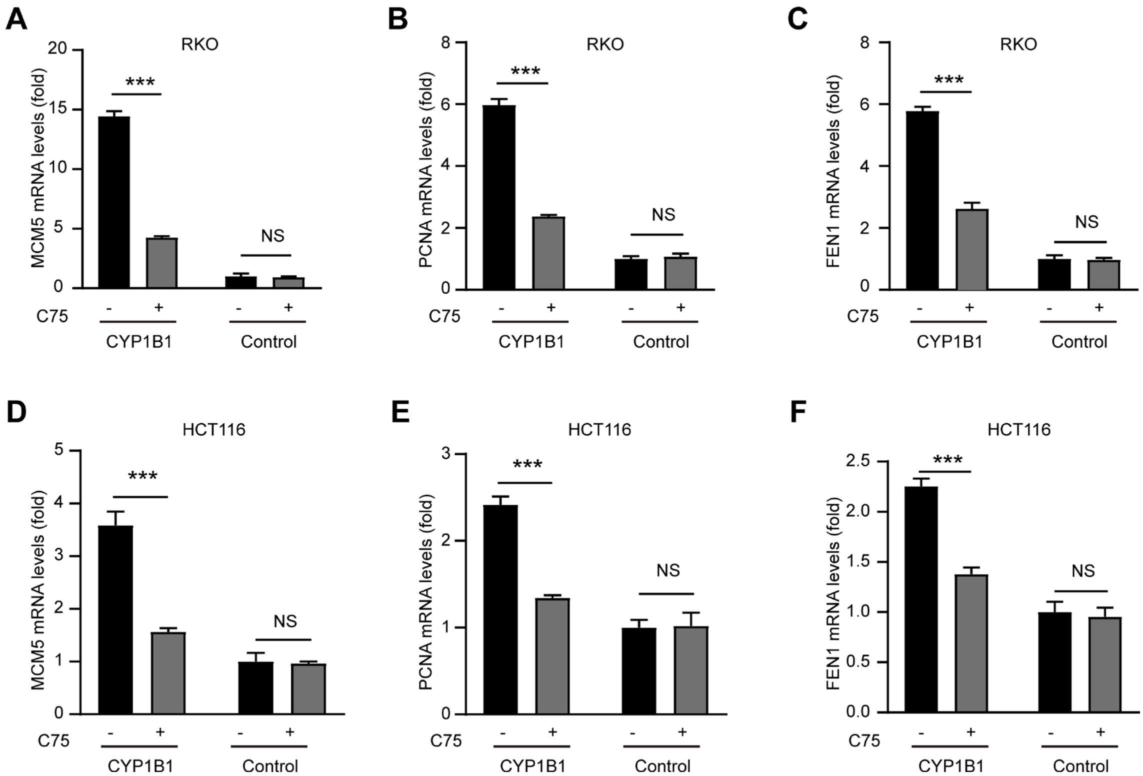

Figure S5 *CYP1B1* promotes CRC cell growth by enhancing fatty acids biosynthesis genes. (A-F) C75 suppresses growth-related genes expression in CRC cells by quantitative RT-PCR. The mRNA levels of MCM5, FEN1 and PCNA in RKO and HCT116 groups were decreased after C75 (10 μM) intervention for 48 h. Representative results from at least three independent experiments are shown. Data are shown as mean ± SD of triplicate. Significance was determined by 2-way ANOVA. ***P<0.001. NS, not significant as indicated. CRC, colorectal cancer; RT-PCR, real-time polymerase chain reaction; mRNA, messenger RNA; SD, standard deviation; ANOVA, analysis of variance.

 https://dx.doi.org/10.21037/jgo-23-895

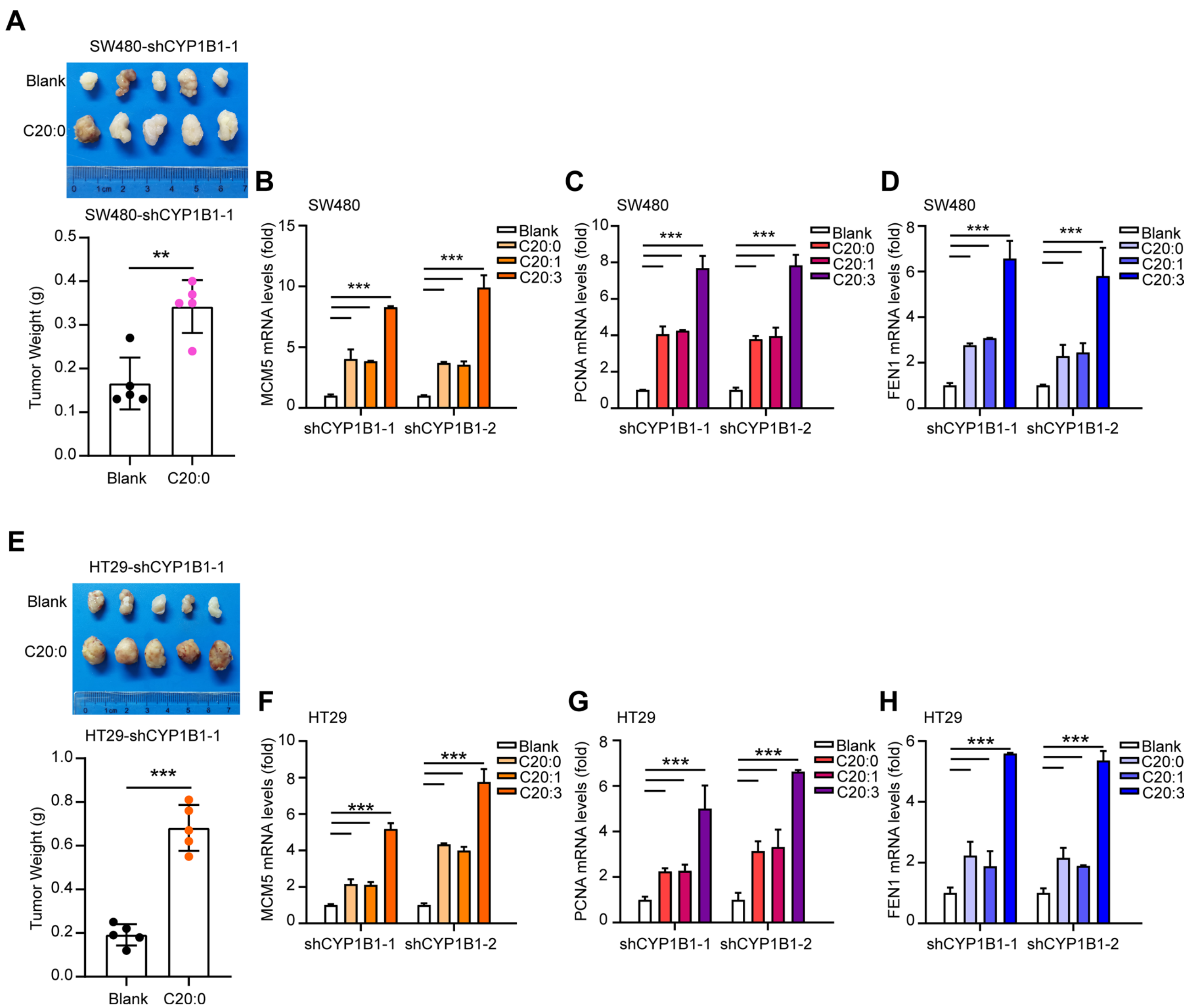

Figure S6 *CYP1B1* regulates the expression of *MCM5*, *PCNA*, and *FEN1* via LCFAs. (A) The effects of C20:0 on tumor growth of CRC xenograft tumors. After co-culture with C20:0 (50 μM, 48 h), 1×10^6 cells were subcutaneously implanted into dorsal right flank of nude mice, tumor volumes were assessed on the indicated days (4 weeks after injection) and tumors were dissected for photo in the up of (A). Data are shown as mean ± SD. (B-D) LCFAs regulate *MCM5*, *PCNA*, *FEN1* up-regulation in SW480 shCYP1B1 cells. After co-culture with LCFAs (50 μM, 48 h), mRNA levels of *MCM5*, *PCNA*, and *FEN1* were up-regulated in SW480 shCYP1B1 cells (B-D). Representative results from at least 3 independent experiments are shown. (E) The effects of C20:0 on tumor growth of CRC xenograft tumors. After co-culture with C20:0 (50 μM, 48 h), 1×10^6 cells were subcutaneously implanted into dorsal right flank of nude mice, tumor volumes were assessed on the indicated days (4 weeks after injection) and tumors were dissected for photo in the up of (E). Data are shown as mean ± SD. (F-H) LCFAs regulate *MCM5*, *PCNA*, *FEN1* up-regulation in HT29 shCYP1B1 cells. After co-culture with LCFAs (50 μM, 48 h), mRNA levels of *MCM5*, *PCNA*, and *FEN1* were up-regulated in HT29 shCYP1B1 cells (F-H). Representative results from at least 3 independent experiments are shown. Significance was determined by Student's *t*-test (A,E) or 2-way ANOVA (B-D,F-H). **, P<0.01; ***, P<0.001. NS, not significant as indicated; LCFAs, long chain fat acids; mRNA, messenger RNA; CRC, colorectal cancer; SD, standard deviation; ANOVA, analysis of variance.

 https://dx.doi.org/10.21037/jgo-23-895